Table of Contents – Chapter III

Page

1.2 Capabilities and Limitations of Current AUT Technology 1

1.2.1 Current Pipeline Girth Weld Ultrasonic Inspection Methods and Techniques 2

1.2.1.1 Amplitude-Based Zonal Discrimination Techniques 2
1.2.1.2 Time-Based Techniques 4
1.2.1.3 Emerging Techniques 6
1.2.1.4 Imaging Techniques 10

1.2.2 Review of Capabilities and Limitations of Current AUT Technology 12

1.2.2.1 Detection Studies 12
1.2.2.2 Sizing Studies 21
1.2.2.3 AUT Advancements 49
1.2.2.4 Pipeline Girth Weld and Repair AUT Inspection Methods – Summary 66
1.2.2.5 References 66

Tables

Table 1.2-1. Comparison of UT Accuracy for All Techniques 30

Table 1.2-2. Relative Ratings of Ultrasonic Sizing Techniques for ID-Connected Cracks 31

Table 1.2-3. Relative Ratings of Ultrasonic Sizing Techniques for OD-Connected Cracks 31

Table 1.2-4. Achieved Height Sizing Accuracy 37

Table 1.2-5. Breakdown of Missed Defects 43

Table 1.2-6. Summary of Performance of Different Techniques 48

Table of Contents – Chapter III (Continued)

Page

Figures

Figure 1.2-1. Mechanized Weld Inspection – Zone Discrimination (Left), and Ultrasonic Channels and Beam Paths per Vertical Zone (Right) 2

Figure 1.2-2. Single-Element P/E Tip Diffraction with A-Scan Display 5

Figure 1.2-3. TOFD Setup and A-Scan Display 6

Figure 1.2-4. Electronic Scanning Resulting from Pulsing a Group of Elements in Sequence Along the Length of PA Probe 7

Figure 1.2-5. Beam Steering (Left) and Focusing (Right) using a PA Transducer Resulting from Specific Delays in the Firing of the Individual Elements in the PA 8

Figure 1.2-6. IDCW with A-Scan Display 9

Figure 1.2-7. Dual-Element Pitch-Catch Tip Diffraction with A-Scan Display 10

Figure 1.2-8. Strip Chart Layout 11

Figure 1.2-9. PISC II Summary Showing POD Results 16

Figure 1.2-10. Example of POD Curve with 40% Threshold 19

Figure 1.2-11. Example of POD Curve with 40% Threshold and TOFD Detection 20

Figure 1.2-12. Example of POD Curve with 20-80% Threshold and Radiographic Detection (New Data Set) 20

Figure 1.2-13. Example of POD Curve with 20% Threshold (Figure 1.2-10 Data Set) 21

Figure 1.2-14. PA Sector Scan of Crack Tip at Multiple Angles (50 to 75 Degrees) 25

Figure 1.2-15. TOFD B-Scan of 1-in.-Thick Carbon Steel Plate with 25% Deep Notch 27

Figure 1.2-16. UT Measurement vs. Actual Height for Thick-Wall Samples 29

Figure 1.2-17. Destructive Flaw Validation – Wide Plate and an Exposed Flaw 34

Figure 1.2-18. Measured vs. Actual Average Height – Approaches A1-A6 and A6A 35

Figure 1.2-19. Height Average Error – TOFD 35

Figure 1.2-20. Depth Average Error – Approaches A1-A6 36

Table of Contents – Chapter III (Continued)

Page

Figure 1.2-21. Length Average Error – Approaches A1-A6 37

Figure 1.2-22. Examples of Defect Height Sizing Errors and Limits Against Undersizing 40

Figure 1.2-23. Distribution of Length and Types of Defect Included in the Tests 41

Figure 1.2-24. The LOF Defect on the Left Fusion Face, at 5 mm from the Outer Surface, was Found by all but One AUT System..... 42

Figure 1.2-25. Defects Associated with Copper in the Weld..... 44

Figure 1.2-26. 3D Data Matrix for all Transmitter and Receiver Combinations 51

Figure 1.2-27. Sector Scan made on a Block with SDH 52

Figure 1.2-28. Elastic Finite Difference Simulation of the TOFD Principle, Showing all the Important Events 53

Figure 1.2-29. Multi SAFT Image (Right) Showing the Result of the LOF Defect (Left) 54

Figure 1.2-30. Strip Chart Display..... 54

Figure 1.2-31. Ultrasonic and Material Parameters 57

Figure 1.2-32. Geometric Parameters and Defect Types 57

Figure 1.2-33. Wave Front is about to Hit Defect..... 58

Figure1.2-34. Reflected Wave Front Just Hit Crystal..... 59

Figure 1.2-35. Amplitude as a Function of Defect Height – Fusion Defect, Corner Effect.... 60

Figure 1.2-36. Beam Intensity on Underbead Defect..... 61

Figure 1.2-37. Reflected Wave Front Just to Hit Crystal..... 61

Figure 1.2-38. Wave Front just about to Hit Defect..... 62

Figure 1.2-39. Example of Round-Robin Test Results on 10-mm-Thick Sleeve (Weld B).... 63

1.2 Capabilities and Limitations of Current AUT Technology

Over the last 15 years AUT has been used increasingly in cross-country and offshore pipeline construction to improve defect detection and sizing reliability. Usually, for practical purposes the main quantities for determination of UT reliability are defect probability of detection (POD) and accuracy of sizing for the defect height and length. A specific requirement for POD that is often used is that it should be at least 90%, when relating to allowable defect sizes at a 95% confidence level (90/95 rule). Very poor POD and sizing results for manual UT (MUT) forced the industry in the mid 1980s and early 1990s to introduce AUT and time-based sizing techniques for inspection of onshore and offshore pipeline girth welds. AUT inspection offers many advantages over conventional MUT including:

1. Improved reliability and performance (defect detection and sizing)
2. Increased speed
3. Ability to obtain an electronic copy of inspection results.

Recently, there has been a strong trend to rely more and more on AUT linear scanning of new construction pipeline girth welds using an array of angle beam shear-wave single-element multi-probes or multi-element PA probes. When using the line scanning approach, an array of probes is attached to the scanner, which is designed to enable the weld to be inspected in one circumferential pass. Multiple transducers, each dedicated for a specific inspection zone, arranged in pulse-echo (P/E) or pitch-catch mode are mounted precisely on a multi-probe scanner head. Typically, 12 to 24 single-element multi-probes or two PA probes are used to inspect the heat-affected zone (HAZ) and the complete weld volume in a single line scan. Once an inspection procedure has been tuned, AUT is inherently very reliable and repeatable. Current approaches for AUT of new construction pipeline girth welds are based on combinations of amplitude-based P/E methods using single-element multi-probes (focused or non-focused) or PA transducers with beam-fixed angles and the time-based time-of-flight diffraction (TOFD) method. For inspection of repair welds and verification of in-service induced non-corrosion-related damage the trends are to apply advanced detection and sizing techniques such as PA electronic (E-) and sectorial (S-) scanning using multiple angles for better detection, advanced imaging, and time-based diffraction techniques for sizing. Although numerous AUT Qualification programs have been performed to determine POD and NDE Sizing Errors these test programs are typically performed for a specific project and the results of the Qualification Program are confidential to the project. There is limited AUT Qualification data in the open literature. Nevertheless the available data clearly confirms that AUT offers significantly improved flaw detection and sizing than MUT.

1.2.1 Current Pipeline Girth Weld Ultrasonic Inspection Methods and Techniques

1.2.1.1 Amplitude-Based Zonal Discrimination Techniques

The amplitude-based zonal discrimination method typically involves dividing the weld into two virtual halves (upstream and downstream) and vertical inspection “zones” approximately 1 to 3 mm in height as illustrated in Figure 1.2-1. The number of vertical zones is dependant on the material thickness, bevel type, and welding procedure. An individual ultrasonic inspection channel is assigned for each zone.

Typically, flat-bottom holes (FBHs) and notches machined in a calibration block and arranged along the specific weld bevel profile are used for calibration targets. Signal amplitude and transit time are setup on these targets. Inspection parameters such as inspection angle, focal spot size, and focal depths are dependent on the weld characteristics and zone geometry. With proper angle beam techniques, echoes returned from the weld zone allow the operator to determine the location, size, and type of discontinuity.

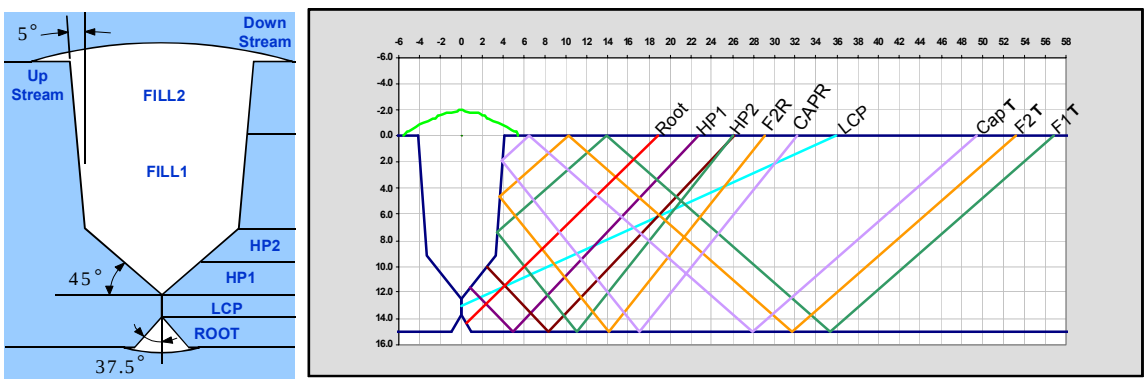

Figure 1.2-1. Mechanized Weld Inspection – Zone Discrimination (Left), and Ultrasonic Channels and Beam Paths per Vertical Zone (Right)

The traditional zonal approach is conservative with some possibilities for over sizing for both multi-probe and PA systems. All efforts to accurately size flaws in the vertical extent using amplitude comparisons are prone to errors because they are based on several assumptions including:

- Flat reflectors smaller than the sound beam diameter
- Simple reflection behavior [FBH, side-drilled hole (SDH), and notch]
- Size increases proportional with the maximum echo amplitude.

Focused Multi-Probes

The use of focused multi-probes with spot dimensions that very closely match the zone height can minimize these errors. For the traditional or simple zone height approach, the accuracy of defect height measurements for bevel fusion zone flaws is achieved only by optimization of beam profile of each single crystal focused probe through variation of radius of curvature (lenses or curved element), element size, and frequency.

A focused probe with a curved element usually incorporates the transducer and replaceable wedge. Each focused probe is designed and fabricated for a specific focal size and focal length (range). Using focused transducers allows the flaw height to be sized with resolution better than the zone height. To increase the POD of sidewall lack of fusion (LOF), the ultrasonic beam should intersect the bevel face at 90 degrees. To determine the exact wedge angle that allows the ultrasonic beam to intersect the bevel face close to perpendicular, velocity measurements are performed for each transducer angle during optimization procedures. Assessment of the vertical extent of sidewall LOF can be improved by observing zonal interaction of signals from zones with smaller heights using beams with similarly small spot sizes. The weld volume is also inspected with focused transducers, but arranged in a different way so that the entire weld volume can be mapped.

Flaw orientation on the bevel is very well known and predictable for pipeline girth welds when the welding is completed by some of automatic methods, e.g., the mechanized gas metal arc welding (GMAW) process. This allows optimization of probe angles and elimination of the influence of misorientation on sizing accuracy in the case of AUT of pipeline girth welds using the zonal approach. At the same time, the zonal concept establishes some uncertainties and inaccuracies for AUT of girth welds. The first uncertainty is related to the beam deflection from the target zone when the diameter of the focal spot is very small (typically less than 2 mm). The small beam results in higher sensitivity of the beam to local differences in ultrasound velocity and surface irregularities. The second uncertainty is related to amplitude “saturation” when the flaw dimension reaches or exceeds the beam size. This situation will reduce the range where there is a linear relationship between flaw size and signal amplitude. To minimize these two uncertainties some procedures adopt a spot size equal to a typical inspection zone, e.g., 3 mm.

Non-Focused Multi-Probes

The P/E non-focused multi-probe approach relies heavily on standard (flat crystal) probes with “natural focusing” of the beam and a beam spot larger than the expected typical flaw height. To reduce the conservatism of the traditional zonal approach, users of non-focused multi-probes reintroduced the amplitude and signature sizing techniques for AUT of pipeline girth welds. By

incorporating a logarithmic amplifier into the AUT system, signals over 100% full-screen height (FSH) in amplitude can be reprocessed without re-inspection of the welds. The so-called amplitude signature denotes the echo-dynamics of each reflection represented in full radio-frequency (RF) waveform (A-scan). It is assumed that the ultrasonic signal from a given flaw is unique based on the full waveform. This technique is used to differentiate "stacked" from inter-zonal flaws detected by two or more transducers and to overcome the disadvantage of the traditional zonal concept to distinguish these two flaws. Stacked flaws occur in two consecutive weld passes or inspection zones in the same circumferential location. If the signatures of a flaw that is detected by two transducers are the same, this flaw is regarded as an inter-zonal flaw. If the signatures are different, the same flaw is regarded as a stacked flaw. Six steps of sizing methodology based on -12-dB amplitude drop technique and signal signature are used to evaluate the flaws.

Recently, there is a practice by users of the P/E non-focused multi-probe approach to treat the hot-pass weld as a single ultrasonic inspection zone. Using this approach, it is possible to miss corner entrapments or make it difficult to evaluate when an indication arises in the middle of the 45-degree bevel, particularly in the vicinity of the original machined weld preparation.

1.2.1.2 Time-Based Techniques

In P/E mode, the signal amplitude is strongly dependent on several secondary factors for all amplitude-based techniques. Apart from the reflector's through-thickness height, the amplitude depends on:

- Angle of incidence of the ultrasonic beam on the reflector
- Roughness of the reflector
- Shape of the reflector
- Position of the reflector with respect to the beam center.

For certain categories of automated welding defects a number of these factors are known. This is the case for LOF and lack of penetration-like defects, which are known to have positions and orientation equal to the original bevel, and are of a more or less predictable shape for some of the automatic welding process. For such defects, the amplitude can serve as a reasonably accurate sizing tool. This is not the case for other defects such as cracks in unpredictable orientations and positions and manual welding defects. Using a time-based technique such as time of flight (TOF) or tip diffraction or so-called recently "back-scattered" technique in one probe arrangement (P/E mode) and TOFD in two probes arrangement (pitch/catch or transmit/receive mode) can compensate for this to a certain extent. TOF and TOFD rely on the diffraction of ultrasonic energies from "corners" and "ends" of internal structures (primarily

discontinuities). When ultrasound is incident upon a linear discontinuity such as a crack, diffraction takes place at its extremities in addition to the normal reflected wave. This diffracted energy is emitted over a wide angular range and is assumed to originate at the extremities of the flaw.

Tip Diffraction

With TOF or tip-diffraction technique using a single probe (single crystal, dual crystal, or PA) in P/E mode, the ultrasonic energy radiating from a crack tip and reflected from the corner is detected and the crack height can then be determined using either absolute or relative measuring techniques.[1.2-1] This technique is possibly the most versatile and widely used in industry. The most difficult aspects of this technique is detecting the relatively weak tip signal and being able to resolve it from the much stronger corner trap signal in A-scan form of presentation (Figure 1.2-2). While shear waves are probably the most common mode of propagation, refracted L-waves are also used to reduce ultrasonic noise caused by the grain structure of some materials.

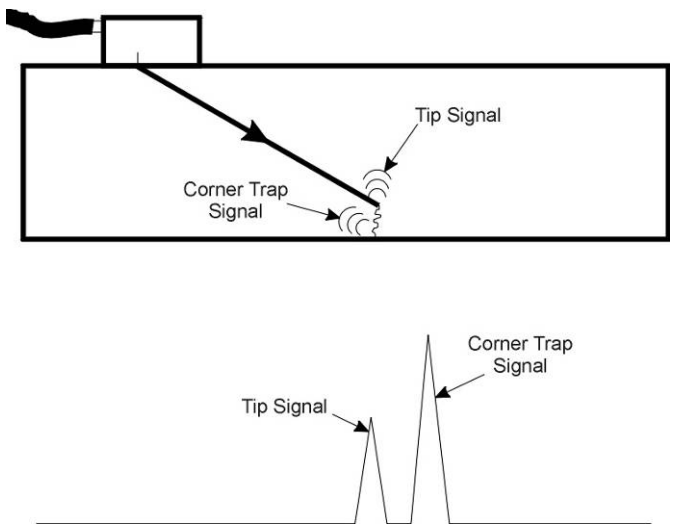

Figure 1.2-2. Single-Element P/E Tip Diffraction with A-Scan Display

TOFD

In addition to energies diffracted by flaws, the TOFD method will detect a surface (lateral) wave traveling directly between the probes and a backwall echo from energies that reach the back of the test piece without interference from defects.[1.2-1] Using this configuration, the depth and through-wall height of the crack can be calculated from simple equations. The study of the TOFD phenomenon has led to the use of this method for:

- Flaw detection as signals may be recorded from a range of flaws
- Flaw sizing since the spatial (or time) separation of the diffracted waves is directly related to the height of the flaw.

The diffracted signals are received via the receiver probe and are evaluated with the ultrasonic system capable to create gray-scale D-scan images. For flaw orientation in a direction vertical to the surface, the size and depth can be evaluated using TOFD (Figure 1.2-3). The time taken for the ultrasonic energy to interact with a flaw tip at a specific depth and return to the specimen is given by a simple equation, and by use of today's advanced computer techniques it is possible to calculate the depth and height of the flaw very rapidly. This makes it possible to perform scans at a relatively high speed that are, in practice, limited only by the mechanics of the system.

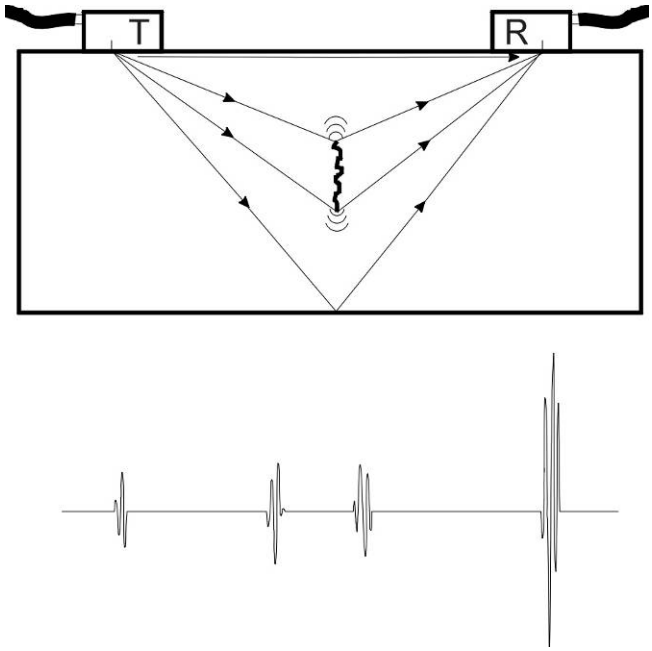

Figure 1.2-3. TOFD Setup and A-Scan Display

1.2.1.3 Emerging Techniques

PA Technology

The angle, focal distance, and focal point size of ultrasound beams generated by conventional UT transducers are fixed by the probe, probe lens, and probe wedge. To generate a different beam angle or focal size, different conventional transducers, lenses, or wedges must be used. In contrast, PA technology can generate a range of ultrasound beams from the same transducer, controlled in real-time by software. The dynamic control of the beam properties and the dynamic depth focusing offers new inspection capabilities not feasible with conventional

transducers. Instead of one crystal, the PA transmit/receive element is split into a set of individual elements. The multiple elements in a PA housing are arranged in linear, rectangular (matrix), or circular (annular and sectored) patterns. Each element of these probes is connected to a different electronic channel, either directly or through multiplexers, depending on the electronic design. Each element can be pulsed or not for each shot. The size and location of the active aperture of the PA probe depends on the activated elements. An electronic delay can be applied to each electronic channel when emitting and receiving the signal to/from the transducer elements. The setup corresponding to all the delays of a given shot is called the delay law (focal law). Each delay law defines a different acoustic beam with a particular direction, focusing distance, and lateral resolution.

The elements in a PA probe can be pulsed simultaneously or in a programmed pattern. “Electronic scanning” is accomplished by pulsing a group of elements electronically in sequence along the length of the transducer. The resulting wave front travels along the length of the PA transducer (Figure 1.2-4). “Beam steering” is accomplished by delaying the pulsing of each element electronically at a set rate. The resulting wave front travels along at an angle dependant on the time delay between firings [Figure 1.2-5 (left)]. “Beam focusing” is achieved by varying the “rate of delay” for the pulsing of each element. The resulting wave fronts propagate toward one another and focus at a programmed distance from the transducer [Figure 1.2-5 (right)]. The actual size of the focal point is determined by the number and size of the elements used. The delay law is computed so that all element contributions interfere at a given point at the same arrival time to focus the beam at a given point for better detection and sizing.

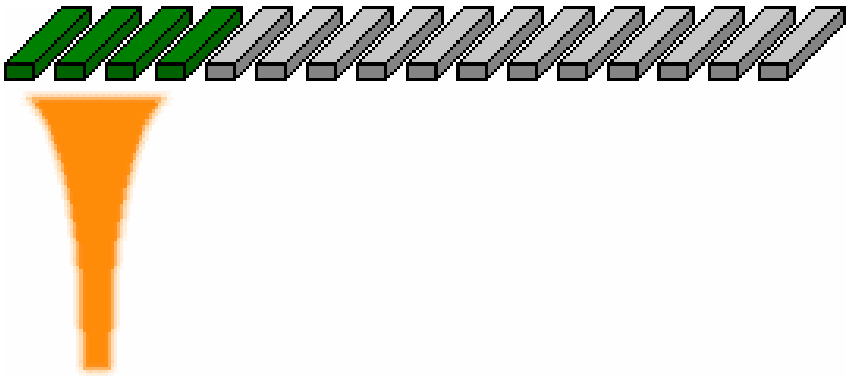

Figure 1.2-4. Electronic Scanning Resulting from Pulsing a Group of Elements in Sequence Along the Length of PA Probe (Courtesy of Imasonic)

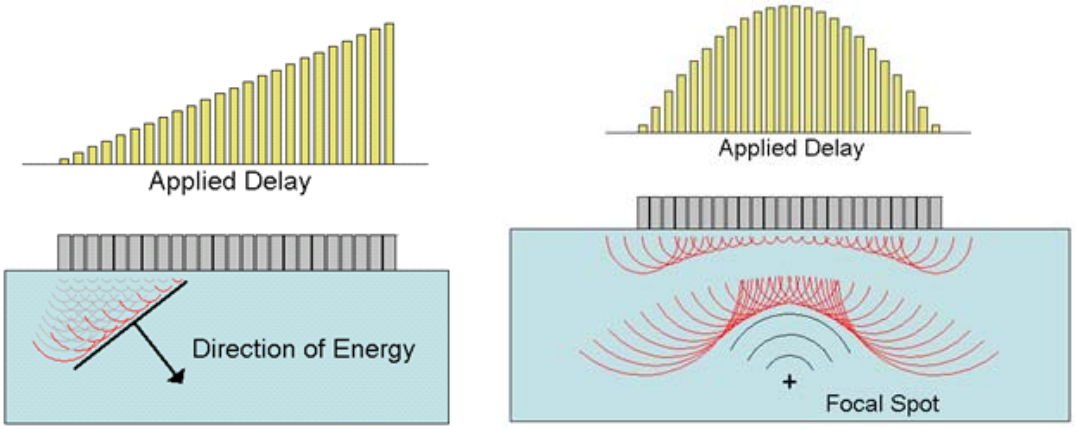

Figure 1.2-5. Beam Steering (Left) and Focusing (Right) using a PA Transducer Resulting from Specific Delays in the Firing of the Individual Elements in the PA

Currently, PA AUT approach for mechanized UT inspection of girth welds is linear PA probes. In addition, this approach is simulating or "mimicking" the multi-probe approach only using focusing PA capabilities and almost ignoring electronic scanning, electronic rastering, electronic steering (sectorial scanning), and advanced imaging and data fusion (merger) capabilities of PA technology. The characteristics of the current PA AUT are the following:

- Traditional zone setup
- Optimized focal law to generate a focused angle beam perpendicular to the bevel
- Limited gate length to the center line
- No cross verification from upstream/downstream sides
- No beam steering in vertical direction
- No sectorial (S-) scan imaging
- No polar view (B-scan cross-sectional circumferential imaging)
- No UT data fusion (merger).

Internal Diameter Creeping Wave (IDCW) Technique

A single-element probe that produces a 70-degree refracted longitudinal wave, a 30-degree direct shear wave, and a 31.5-degree indirect shear wave is used for IDCW. The technique is often referred to as the "30-70-70" technique, getting its name from the 30-degree shear wave which mode converts to a 70-degree longitudinal wave when it strikes the opposite [inside diameter (ID)] surface. The resulting wave then reflects off a crack face and back to the transducer at an angle of approximately 70 degrees.

The other signals produced by the probe are also very useful for detection and sizing of ID-connected cracks. For example, the 31.5-degree wave mode converts upon hitting the opposite surface to produce a longitudinal IDCW. This wave is very sensitive for detecting the presence of ID connected flaws. In addition to the direct and indirect shear waves, the 70-degree refracted longitudinal wave (L-wave) can be used to look for cracks having a height equal to 50% of the wall thickness or greater.

The major disadvantage of the IDCW technique is interpretation of the A-scan signals shown in Figure 1.2-6. While much information about crack height can be gained from this technique, the ultrasonic inspector must be very familiar with ultrasonic wave propagation principles in order to properly interpret the displayed signals.

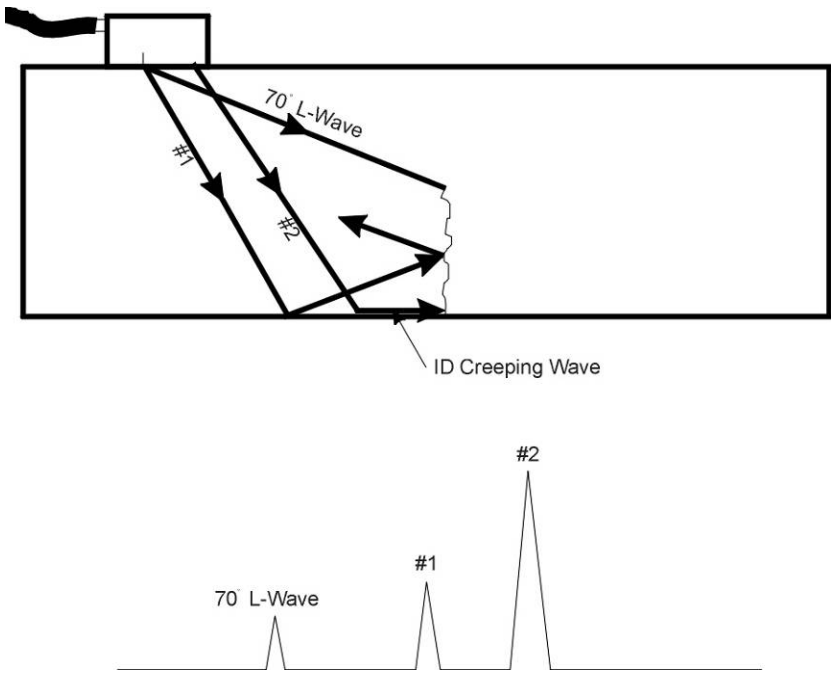

Figure 1.2-6. IDCW with A-Scan Display

Dual-Element Pitch Catch Technique

Dual-element probe that consist of a single-probe housing containing two elements in a pitch-catch (transmit-receive) angle-beam arrangement is used for this technique (Figure 1.2-7). These transducers are available with the elements in a side-by-side or tandem arrangement. Depending on the angle of transmit and receive elements, the dual-element technique basically allows the use of P/E techniques to be used in a pitch-catch arrangement. Other tip-diffraction techniques, as well as IDCW, can all be performed with a dual-element probe.

The primary advantage of dual-element probes is the ability to focus the sound energy at a predetermined depth within the material. Focusing is achieved by angulations of the elements by the transducer manufacturer and is fixed for each transducer. By focusing the sound beam, it is often possible to obtain a better signal-to-noise (S/N) ratio in large-grain materials such as austenitic steels. In such situations, dual-element probes can often help distinguish a crack tip from surrounding grain noise.

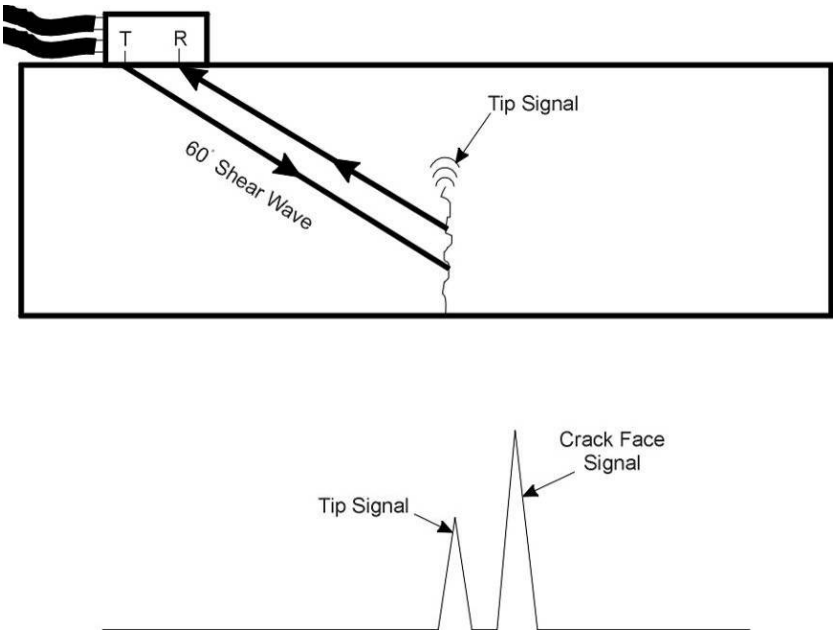

Figure 1.2-7. Dual-Element Pitch-Catch Tip Diffraction with A-Scan Display

1.2.1.4 Imaging Techniques

Although there are some differences in current AUT approaches, all of them provide similar information that can be used for flaw size measurements. The following information on indications found in a weld is available as a basis to establish the through-thickness size of reflectors:

- Location of zones and number of zones in which the indications are detected.
- Signal amplitude (A-scan representation) of indications in one zone or several different zones detected by P/E or pitch/catch channels.
- Volumetric image (D-scan color representation) of indications in root and cap zones detected by mapping P/E channels.

- TOFD image (D-scan gray representation) showing upper and/or lower tip of the reflector (dependent on the reflector's nature and location).

Currently, only two of the basic ultrasonic data display techniques are implemented in the field AUT systems customized for girth weld inspection. A-scan which is the basic ultrasonic waveform data displayed as amplitude of the reflected sound energy versus the TOF of the ultrasonic wave and D-scan which is a graphical representation of the ultrasonic data where the TOF of the ultrasonic wave is plotted against the probe travel position. For weld inspection D-scan is normally a cross-sectional view along the weld length.

All commercially available AUT software for girth weld inspection comprises a module that is capable of performing disposition of indications against a code or standard, including through-thickness sizing and application of defect interaction rules. UT data is displayed in multiple views using proprietary graphical-user interface displays almost identical for the current approaches. Each inspection zone is represented by multiple sets of vertical strips displaying amplitude, TOF, couplant, and volumetric mapping data. The strips are labeled with the inspection zone symbol and form a so-called strip chart (see Figure 1.2-8). Unique features and color spectrum provide support to the operator for rapid identification of amplitude and TOF, flaw characterization, calculating the high and length, and electronic marking. A ruler is incorporated also in the screen window to indicate the circumferential location of UT indications. In addition, TOFD data is presented in gray scale on the screen and can be used for vertical sizing or to evaluate misaligned and off-axis defects.

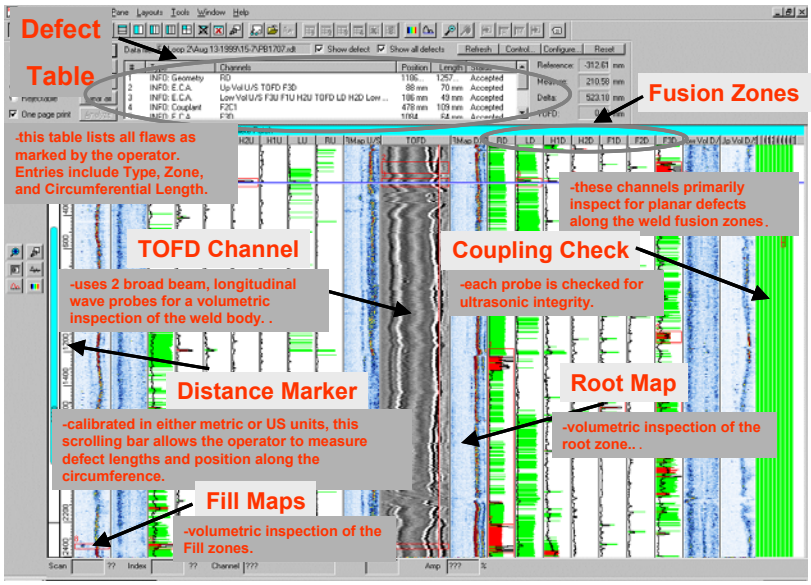

Figure 1.2-8. **Strip Chart Layout** (Courtesy of Canspec, Canada)

Data gathered by PA can be displayed using any combination of A-scan, B-scan, C-scan, D-scan or sector (S-scan) and polar view in multi-screen views. Despite that the combination of multiple angles, focal points, and data-analysis tools gives the user a wealth of information for evaluating of flaws is still not available in AUT systems for onshore or offshore pipeline girth weld inspection.

1.2.2 Review of Capabilities and Limitations of Current AUT Technology

The capabilities of AUT systems to detect and size flaw differs with changes in variables like pipe material, thickness, weld bevel, inspection procedures, data presentation, to name a few.

There have been many studies performed for evaluation of various AUT setups for various applications. This section includes review of capabilities and limitations of current technologies reported on several studies performed for specific use. This section also discusses the recent advancement that is taking place in the field of AUT.

1.2.2.1 Detection Studies

It was found that very limited results are published in the open literature from studies related to flaw-detection capabilities and POD of AUT.

Study 1 – Ultrasonic Cracks Detection Limits[1.2-2)]

Crack detection using UT, depends on the reception of sound energy being reflected and diffracted from a crack. The larger the reflecting surface of the crack, the greater will be the chances of detection. Therefore, crack size, both depth and length, have a direct bearing on detectability. In addition, since sound energy is attenuated as it travels through a material, component thickness is also a major factor. To say that a 0.05-in. (1.3-mm)-deep crack can be detected, is not very meaningful unless the material thickness is also known. For example, detection of a 0.05-in. (1.3-mm)-deep crack in a 0.5-in. (12.7-mm)-thick component is realistic; however, detection of the same size crack in an 8-in. (203-mm)-thick component would be doubtful. Consequently, it is useful to view crack-detection capabilities in terms of the percentage of part thickness.

Ultrasonic crack detection is a two-fold situation. First, the crack must be detected and second, it must be properly interpreted as a crack in order to prevent unnecessary repairs. For example, when an ultrasonic indication is detected, it must be determined if the indication is from a corner-trap condition caused by a surface-breaking crack or a false indication caused by weld geometry or surface imperfections. In order to differentiate between a crack and a false

indication, it is important to be able to detect and resolve the crack tip, which is normally a much lower amplitude signal. This means that surface-breaking cracks may be detectable because of the relatively strong corner trap signal; however, the inspector may not be able to correctly identify the indication as a crack unless a tip signal can be detected or another nondestructive testing (NDT) method confirms the presence of a crack.

The uncertainty of defect classification can be seen in a POD study by Doctor *et al*.[1.2-3] One aspect of the study was to look at POD of fatigue and intergranular stress-corrosion cracking (IGSCC) in 10-in. (254-mm)-diameter Schedule 80 stainless steel pipe using MUT. The study showed that the probability of detecting the presence of a discontinuity ranged from approximately 50% POD for a 10% through-wall crack to approximately 70% POD for a 50% through-wall crack. On the other hand, the probability of detecting and properly classifying the discontinuity as a crack was approximately 20% for a 10% through-wall crack and approximately 50% for a 50% through-wall crack.

Because of weld effects such as bead geometry and variations in grain structure, it follows that crack-detection capabilities in weld zones will be worse than those encountered in un-welded base metal. Some literature gathered during this project shows what is achievable under nearly ideal conditions. This is useful information for establishing a minimum threshold for detectability under the best of conditions.

Theoretical Detection Limits

Bowker *et al*.[1.2-4] provide a means for calculating the minimum height of a through-thickness planar flaw that can be resolved. It should be noted that it is possible to detect smaller flaws even though the flaw may not be sized.

$$H = \frac{n\lambda}{4(\cos\theta)} \tag{1-1}$$

where:

H = Minimum through-thickness resolution
n = Number of cycles in pulse train
λ = Ultrasonic wavelength
θ = Refracted beam angle

Silk reports that for long shallow cracks, less than 1/5 λ_L through-wall height, there is little interaction between the ultrasonic wave and the crack.[1.2-5] This means that there is virtually no reflected signal when the crack height is less than or equal to 1/5 of the longitudinal wavelength. Between 1/5λ_L and 1/2λ_L there is a rapid increase in the reflected signal from the crack. At crack heights greater than 1/2λ_L the reflected signal increases in a linear fashion until the crack dimensions approach those of the receiver element. At crack dimensions greater than the dimension of the receiver element, little or no increase in reflected signal would occur. To put this in perspective, consider the following example:

- Material = carbon steel
- Longitudinal wave velocity (V) = 5800 m/s (0.230 in./s)
- Test frequency (f) = 5 MHz

$$Wavelength(\lambda_L) = \frac{V}{f} = 1.17\ mm\ (0.046\ in.) \rightarrow \frac{\lambda_L}{5} = 0.23\ mm\ (0.0092\ in.) \rightarrow \frac{\lambda_L}{2} = 0.58\ mm\ (0.023\ in.) \quad (1\text{-}2)$$

Silk states that "for cracks … theory suggests that detection will be unreliable for depths less than λ_L /2 and virtually impossible for depths of λ_L /5 or less".

Silk makes an interesting observation that while the rapid drop in reflected signal for cracks occurs at approximately λ_L /2, the same rapid drop for cylindrical SDH does not occur until the diameter of the hole is equal to or less than λ_L /8. One can see that for crack heights less than λ_L /2, a comparable size SDH will produce a larger reflected signal. Since SDH are often used as artificial reference reflectors, it is important to be aware of this relationship.

Case Studies

According to Taylor *et al*. round-robin study the minimum resolution that would be expected in austenitic stainless steel would be 0.040 in. (1 mm) using 5 MHz.[1.2-6] The study was performed to look at the inspection performance for detecting and sizing IGSCC in austenitic stainless steel pipe. Both manual and advanced UT methods were evaluated during the study. The smallest crack used in the study was 0.030-in. (0.76-mm) deep in a 0.500-in. (12.7-mm)-thick pipe wall (6% through wall). The authors point out that "if a test frequency of 5 MHz is used, cracks 0.040 in. (1 mm) or less would appear like blank material (un-cracked) with crack-like signals." It follows then, that trying to detect cracks of this size would tend to increase the number of false calls. One interesting conclusion from this round-robin study was that no significant difference

in the POD performance was found based on crack length for IGSCCs. Long cracks in the range of 3 to 40 in. (76 to 1016 mm) were detected at approximately the same rate as cracks that were less than 2-in. (50.8-mm) long.

Cerri and Cusolito performed detection studies on samples of welded 304 stainless steel pipe having diameters of 12 to 24 in. (305 to 610 mm) and wall thickness ranging from 0.5 to 1 in. (12.7 to 25.4 mm).[1.2-7] The results show that electro-discharged machining (EDM) notches and IGSCCs having a through-wall height as small as 5% were detected with a POD of approximately 90%. All flaws were ID connected. Good detection was achieved using 1.5- to 2.25-MHz transducers with a refracted shear-wave beam angle of 45 degrees. It was noted that at a 60-degree beam angle, several of the shallow flaws were missed. It was theorized that the 45-degree shear wave took better advantage of the reflected sound energy from the corner trap effect, caused by surface-breaking flaws, than did the 60-degree shear wave. The best detection capability in the study, however, was achieved using a 30-70-70 IDCW probe. The creeping-wave probe exhibited POD numbers slightly higher than conventional P/E probes.

Nishino *et al.* conducted research on welds in 3.15-in. (80-mm)-thick cast stainless steel (18 Cr-8 Ni) using a 1-MHz probe having a 45-degree refracted longitudinal beam.[1.2-8] The report states that slits, used to represent cracks, were detected when the slits were greater than 5% of the wall thickness [> 0.16 in. (4 mm) in through-wall height]. The slits were placed on the inner wall to represent surface-breaking cracks in the HAZ near the root of the weld. In the same report, machined slits and cracks having through-wall heights greater than 10% of the wall thickness were detected in the HAZ of drawn tube welds. The welds were U-groove welds in material that was 0.55- to 1.42-in. (14- to 36-mm) thick. In order to detect the cracks, a 4-MHz probe was used with a 45-degree shear-wave beam. One of the observations noted during the project, was that the ultrasonic echo amplitudes from cracks were sometimes less than half the amplitude of the machined slits used to simulate cracks.

Increases in sensitivity can often improve detectability but will also result in a larger number of miscalls. Work performed in the Program for the Inspection of Steel Components (PISC) projects show that it is advisable to work at a medium amplitude cutoff level.[1.2-9] For example, it was observed that a 20% of distance amplitude curve (DAC) amplitude was a sufficient cutoff point for obtaining good detection without an increase in the number of false calls when using the ASME Section XI calibration procedure. On the other hand, smooth fracture face cracks with sharp crack tips, such as fatigue cracks, were almost never detected, regardless of depth, when using 50% DAC cutoff.

In the PISC II report, an inlet nozzle of a PWR pressure vessel was ultrasonically inspected for surface and sub-surface cracks. The material was SA533 B Class 1, having a thickness of

approximately 10 in. (254 mm). The cracks were service-induced cracks having both smooth and rough surface fracture faces. The reported crack dimensions were 0.12 to 2.36 in. (3 to 60 mm) in through-wall height (depth), by 0.12 to 3.35 in. (3 to 85 mm) in length. The vessel was inspected by several teams of ultrasonic inspectors using inspection requirements that were "in the spirit of ASME". The best POD from each team was reported and is shown in Figure 1.2-9.

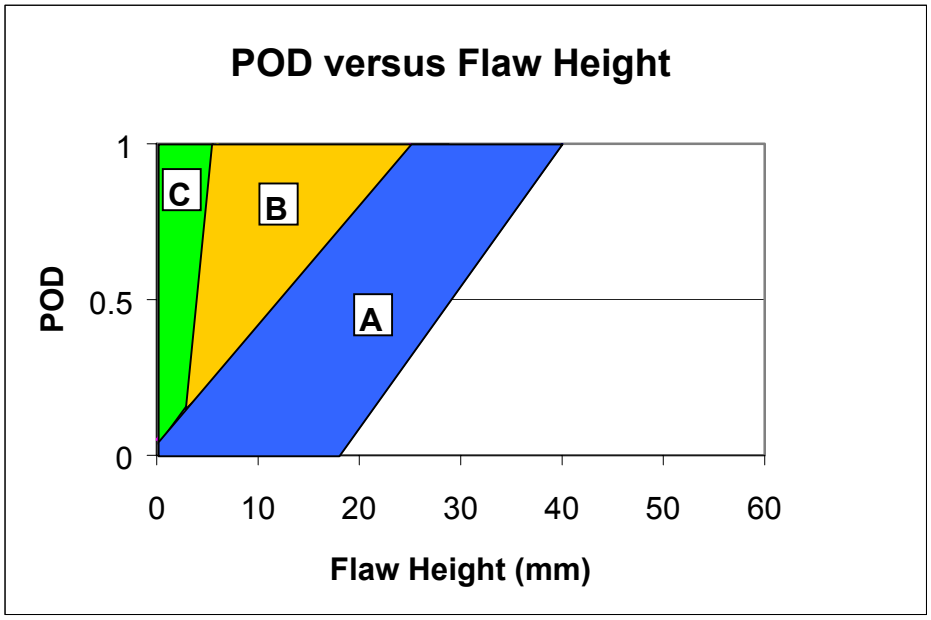

A : Smooth Cracks With Sharp Crack Edge
B : Rough Defects or Defects with Large Crack Edges
C : Volumetric Defects

Figure 1.2-9. PISC II Summary Showing POD Results

Shackleton *et al.* report detection of through thickness planar flaws 0.06 in. (1.5 mm) in height in a C-Mn pressure vessel having a wall thickness of 3.35 in. (85 mm).[1.2-10] The flaws were located in the fusion boundary between the weld and base metal. The report states that detection was accomplished using a 4-MHz probe with a refracted beam angle of 45 degrees. It is not clear from the report if the beam angle was a refracted longitudinal wave or a shear wave. While the detection of flaws having a through-wall height of less than 2% is very good, the report goes on to say that there were approximately the same number of false calls as there were correct calls.

Shannon *et al*. were able to detect cracks as small as 0.02 in. (0.5 mm) in through-wall height in carbon steel pipe having a wall thickness of 0.39 in. (10 mm) (5% of the wall thickness).[1.2-11]

The testing was performed as an in service inspection, using an inspection pig. From the article it appears that a large number of false indications were also encountered and work was being done to reduce false indications using electronic filtering and signal processing.

Signal processing techniques may help for crack detection in materials that have a high noise level. In a study involving ultrasonic inspection of 0.55-in. (14-mm)-thick austenitic stainless steel welds, Raj and Subramanian were able to detect an EDM notch having a through-wall height equal to 5% of the material thickness, without signal processing.[1.2-12] They report that notches less than 5% in through-wall height could not be detected. After applying signal processing techniques on the acquired data, notches and natural flaws having a through-wall height of approximately 1% were detected. The signal processing techniques consisted of a combination of pattern recognition and cluster analysis of magnitude and position.

In clad vessels, Charlesworth and Hawker report detection of cracks in the clad layer using TOFD while inspecting from the clad surface.[1.2-13] They were not able to obtain accurate sizing, however, until the crack had propagated 0.24 in. (6 mm) beyond the clad interface. In a similar TOFD study on a clad nozzle, Stringfellow and Perring report the lower limit of detectability to be approximately 0.12 in. (3 mm) and that a crack depth of greater than 0.20 in. (5 mm) was needed to obtain sizing information.[1.2-14] This agrees well with a paper by Trimborn that reports the detection of scan side surface-breaking cracks having a through-thickness height of 0.08 in. (2 mm).[1.2-15] In the English translation of the Trimborn report the type of material is not listed but is assumed to be carbon steel.

Lemaitre *et al.*[1.2-16] report that EDM notches greater than 10% of the wall thickness were consistently detected during PISC III round-robin evaluations in the weld and HAZ of wrought-to-cast stainless steel welds in 2.68- to 3.23-in. (68- to 82-mm)-thick material. Similar results were also reported for surface-breaking fatigue cracks and EDM notches in the weld and HAZ of cast-to-cast austenitic steel welds. Many ultrasonic techniques were used including P/E, dual-element, TOFD, SH waves, and creeping waves. In at least one instance, the synthetic aperture focusing technique (SAFT) was used to help analyze the TOFD data. However, regardless of the technique used, through-wall planar flaws less than 10% of the thickness were difficult to detect.

Davis[1.2-17] reported the best detection found in the literature review. Using a 4-MHz, IDCW (30-70-70) probe, a 0.005-in. (0.13-mm)-deep EDM notch (0.5% of the wall thickness) was detected in 1-in. (25.4-mm)-thick carbon steel. The S/N ratio was reported to be approximately 4:1. Based on other case studies, as well as, the theoretical limitation of ½ the longitudinal wavelength reported by Silk, this would be an example of a “best-case” scenario for limited data without POD study.

Conclusions

Based on the cases reviewed, welds and HAZ cracks need to have a through-wall height approximately 5 to 10% of the material thickness before they can be reliably detected. Cracks in carbon steel can generally be detected if their through-wall height is 5% or more, while cracks in austenitic stainless steel welds need to be closer to 10% in through-wall height.

Except for the slightly better detection performance reported for the IDCW (30-70-70) technique; all techniques were similar in crack detection capabilities. However, when comparing MUT to AUT inspection, Hands reports that manual inspection may have a slight advantage in overall sensitivity; however, when signal processing and test reproducibility is considered, he says that automated UT techniques can provide superior performance.[1.2-18]

Signal processing appears to improve detection capabilities in material having a high ultrasonic noise level. These techniques help primarily by reducing the ultrasonic noise to a level where crack signals can be seen.

Factors such as crack depth, crack orientation, and fracture face roughness appear to influence detectability; however, crack length does not appear to be a significant factor provided adequate sound energy can be reflected from the crack face or corner trap.

When comparing the signal amplitude of artificial flaws to the signal amplitude of cracks, the signal amplitude of cracks will be significantly less. In fact, the literature shows that signal amplitude differences of at least 6 dB (2×) are common.

Study 2 – AUT of Girth Welds POD Curves[1.2-19]

Limited generic examples for POD curves based on results AUT of girth welds offshore qualification trials were reported by Forly.[1.2-19] Currently, AUT of girth welds qualification trials are conducted project by project and details related to specific AUT systems, procedures, and results are confidential. Because of the confidentiality it is difficult to make conclusions for the POD performance of multi-probe or PA AUT systems and related procedures. Figure 1.2-10 shows a typical example of an AUT POD curve with 40% FSH threshold when sensitivity settings are based on 80% FSH response of 3-mm FBH on the bevel. Figure 1.2-11 shows a typical example of an AUT POD curve when P/E criteria is supplemented by TOFD detection. Adding an additional detection technique such as TOFD to the primary P/E detection technique leads to reduction of 90/95 POD height from 2.2 to 0.7 mm.

An example of POD curve variation depending on recorded echo amplitude threshold for the same data base and detection criteria is shown in Figure 1.2-12. Included in the same graph for comparison is a radiographic detection curve for wall thickness range 16 to 20 mm.

Figure 1.2-13 shows an example of a different set of data and detection criteria. Reduction of the threshold level from 40% FSH to 20% FSH when sensitivity settings are based on 80% FSH response of 3-mm FBH on the bevel improved 90/95 POD height for the primary P/E detection technique to 1.26 m.

It was found to be more advantageous and could improve the POD if the information from multiple channels and techniques are used more actively for cross verification of detected flaws. It was recommended to use TOFD information in addition to P/E and the detection information from the mapping channels.

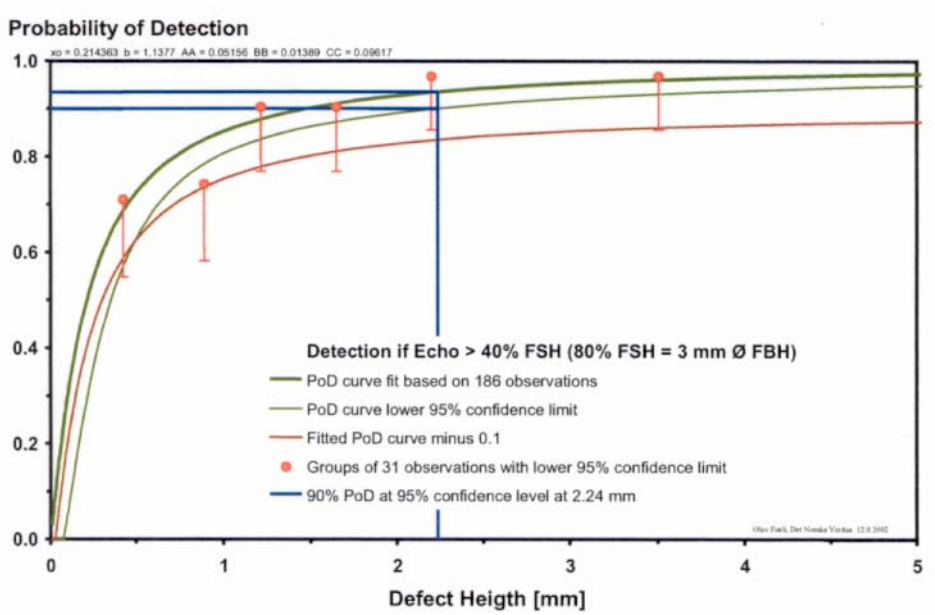

Figure 1.2-10. Example of POD Curve with 40% Threshold (Courtesy of DNV)

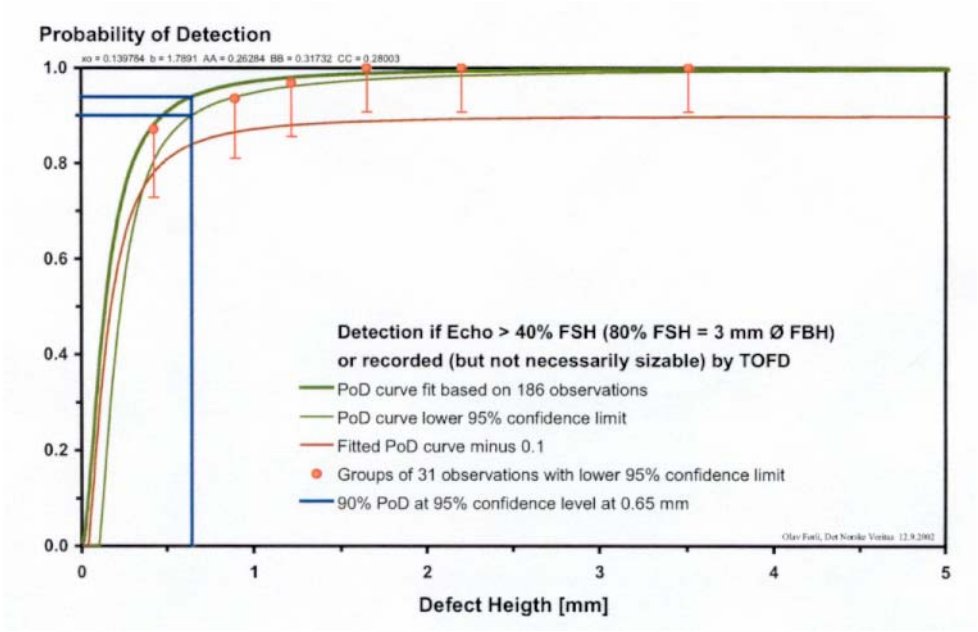

Figure 1.2-11. **Example of POD Curve with 40% Threshold and TOFD Detection** (Courtesy of DNV)

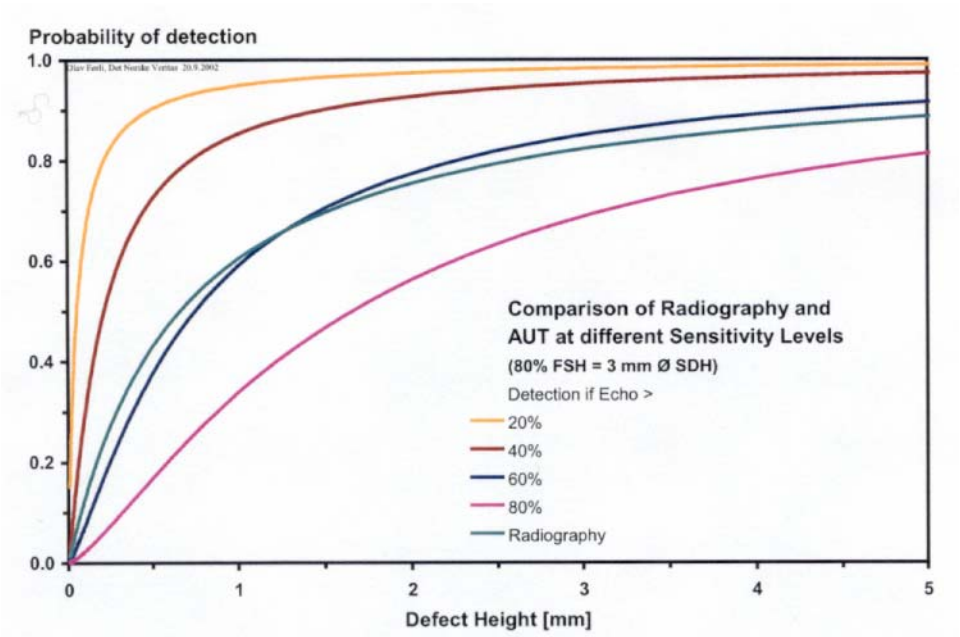

Figure 1.2-12. **Example of POD Curve with 20-80% Threshold and Radiographic Detection (New Data Set)** (Courtesy of DNV)

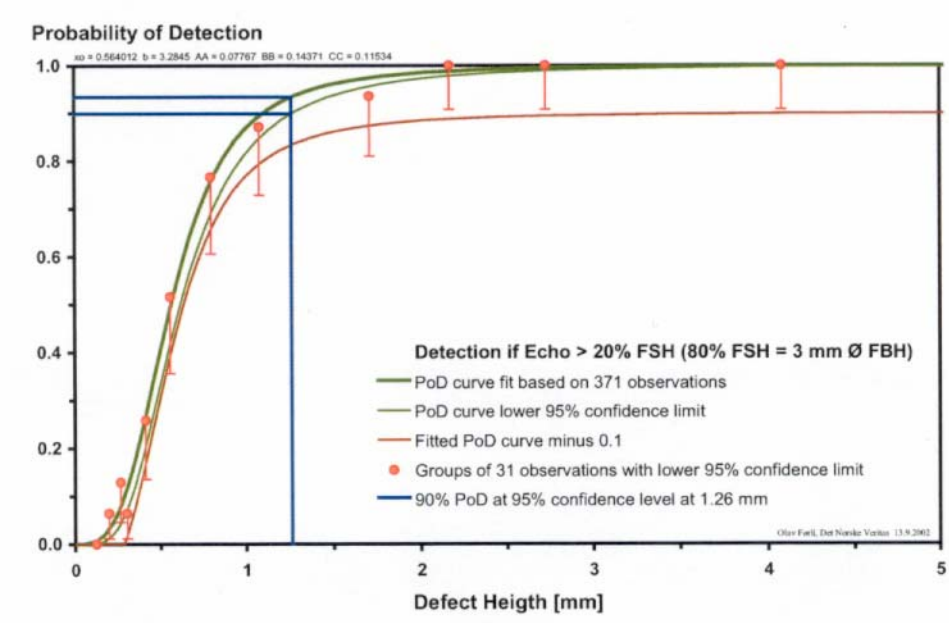

Figure 1.2-13. Example of POD Curve with 20% Threshold (Figure 1.2-10 Data Set) (Courtesy of DNV)

1.2.2.2 Sizing Studies

Study 3 – Ultrasonic Height Determination of Cracks[1.2-20]

This study concentrated on ultrasonic sizing techniques for surface-breaking cracks.[1.2-20] Five techniques were selected based upon their popularity and success for sizing cracks. All five techniques hinge upon detection of the crack tip, which has proved to be a very accurate approach to measure crack height.

Since crack height is of more importance than crack length, from a fracture mechanics viewpoint, this project concentrated largely on crack height measurements rather than crack length. The reasoning behind this is that ultrasonic measurements of crack length are basically limited to the popular “6-dB drop” techniques. These techniques have been used successfully for many years as good indicators of crack length, provided the crack can be accurately detected.

The experiments were conducted in two phases. During the first phase, all five techniques were compared against each other to determine the attributes of each. In the second phase, samples having unknown crack heights were tested using applicable techniques. Selected samples were then cross sectioned and actual crack heights were compared to the ultrasonic estimates.

All five ultrasonic techniques were compared on 25-mm (1-in.)-thick carbon steel samples containing controlled cracks. The sample thickness of 1 in. was chosen so that all five techniques could be evaluated on the same reflectors. Each technique, in one form or another, relies on detection and resolution of the crack tip. The results of the comparisons are discussed in the following sections.

Evaluation of IDCW Technique

The IDCW technique proved very good at detecting cracks originating on the surface opposite the inspection surface. Using the IDCW technique, 0.005-in.-deep EDM notches have been detected in 1-in.-thick carbon steel, with an S/N ratio of better than 4:1. Although detection capabilities are excellent, sizing cannot be done with the precision of some of the other techniques. This, however, does not lessen the usefulness of the technique.

IDCW is a good technique to approximate crack height prior to using other techniques. Once an operator can determine the approximate through-wall height of a crack, the appropriate technique can then be selected in order to gather more precise measurements.

As cracks deviate from being perpendicular to the surfaces, crack height estimates could be in error. These errors will occur primarily for cracks that have a height in the range of 20 to 50% of the thickness.

Although the IDCW technique is normally used for ID-connected cracks, it is also useful for sizing deep cracks originating from the outside diameter (OD) surface. The 70-degree refracted L-wave and the 30-degree direct shear wave can be used to approximate the crack height of OD-connected cracks in much the same way as it is used for ID-connected cracks.

Evaluation of Single-Element P/E Tip-Diffraction Technique

The single-element, P/E tip-diffraction technique is possibly the most versatile and least expensive of the five techniques. It also does not require the training and experience of some of the other techniques, but a skilled operator is still essential for obtaining accurate results. Test results from this study show that single-element tip diffraction sizing worked well for cracks originating on either the scanning surface (outer surface) or the opposite surface (inner surface). Likewise, single-element tip diffraction works well for sizing cracks of any reasonable depth provided the crack-tip signal can be resolved from the corner trap signal.

For best results, parameters such as sound beam angle, transducer size, and frequency is required to be optimized. In order to evaluate these parameters, experiments were conducted

on 1-in.-thick carbon steel samples containing saw-cut notches and fatigue cracks having through-wall heights up to approximately 75% of the wall thickness. The results from these tests show that shear-wave techniques are much better at detecting crack tips than refracted L-waves. While refracted L-waves offer better penetrating power for thick materials and reduced noise level for large grain materials, the longer wavelengths are a disadvantage for crack-tip detection.

As would be expected, transducer size and frequency have a significant affect on crack tip resolution primarily because of beam spread. The frequency needs to be high enough to detect fine cracks and yet low enough to penetrate through the material with an acceptable S/N ratio. For most crack sizing applications, a frequency of 2 to 5 MHz works well; however, to improve resolution a higher frequency is desirable. A slightly lower gain setting was used for the 2.25-MHz transducer but resolution is significantly decreased. In addition, the slight increase in beam spread combined with the longer wavelength of the 2.25-MHz transducer produces a higher amplitude corner trap signal that can mask nearby tip signals.

Transducer size needs to be large enough to generate sufficient sound energy in the material and small enough to obtain accurate sizing in areas that may have limited access. ¼-in.-diameter transducer produces a higher amplitude signal from the crack tip with an improved S/N ratio. As material thickness increases though, a larger transducer element is needed in order to generate sufficient sound energy with reduced beam spread.

One other important factor in tip diffraction sizing is selection of beam angle. In the comparison tests conducted in 1-in.-thick carbon steel, lower shear-wave angles in the range of 45 to 60 degrees worked well for crack-tip detection of shallow cracks propagating from the opposite surface that were $^{1}/_{16}$- to ½-in. deep. The S/N ratio was found to be much better with the 60 degrees than with the 45 degrees (6:1 vs. 2:1) when using the same transducer. Shear-wave angles in the range of 60 to 70 degrees generally worked well for deeper cracks that were ¼- to ¾-in. deep from the opposite surface. When using a 45-degree shear-wave angle to size cracks propagating from the opposite surface, crack tips greater than ¼-in. deep were difficult to detect. Conversely, when using a shear-wave angle of 70 degrees, crack tips less than ¼-in. deep were difficult to detect. Shear-wave angles in the range of 53 to 60 degrees generally provided a good compromise for detecting crack tips throughout the 1-in. thickness. Corner trap signal can be seen at 60 degrees but not at 70 degrees.

Tests were also conducted on cracks open to the scanning surface. The results show a significant difference between viewing the crack tip on the first leg (prior to the sound beam reflecting off the back surface) and viewing the crack tip on the second leg (after the sound beam has reflected off the back surface). When using first leg data, shear-wave angles of 60 to

70 degrees worked well at detecting crack tips ranging from ¼ to ¾ in. in height. When using second-leg data with the same probe, shear-wave beam angles of 45 to 60 degrees proved to be best at detecting the crack tips. In cases where the crack was less than ¼-in. deep; however, angles of 55 to 60 degrees did a better job of resolving the crack tip on the second leg. Shear-wave techniques with angles greater than 60 degrees did not perform well when looking at second-leg data.

Evaluation of Dual-Element Pitch-Catch Technique

The dual-element, pitch-catch evaluations, conducted during this study, perform well at the focal depth of the transducer, but the accuracy decreases as the crack-tip depth deviates from the transducer focal depth. This is primarily due to the angle of the transmitter and receiver elements. By angling these elements, the transducer manufacturer can focus the sound beam at a predetermined depth; however, the angled elements induce inaccuracies into crack height measurements. Inaccuracies in height measurement are the result of the non-linear relationship between TOF and through-wall depth. This is the same non-linear relationship noted for the TOFD technique. Some compensation can be made by calibrating the ultrasonic instrument to measure at a specific depth within the material; however, as the actual depth of the crack tip deviates from the calibrated depth, inaccuracies will be encountered. As long as dual-element probes are used for crack sizing at their designed focal depth, the accuracy will be similar to P/E techniques, but this assumes that the approximate crack height is already known.

As mentioned previously, a major advantage of dual-element probes is the ability to distinguish crack tips in “noisy” material. This allows techniques such as IDCW and tip diffraction to be used in situations where the S/N ratio would otherwise prohibit the use of these techniques. These techniques are possible by using a special type of dual-element probe known as a bi-modal probe. As the name implies, bi-modal probes use a combination of high-angle longitudinal waves and low-angle shear waves to determine crack height. During this study, the bi-modal technique was not evaluated.

Evaluation of PA Tip-Diffraction Technique

The PA tip-diffraction technique is excellent for determining crack height. When compared to conventional tip diffraction, the accuracy of PA in these tests was similar; however, the ability to display the data in a variety of ways greatly enhances the operator’s ability to distinguish crack-tip signals from non-relevant signals.

While the technique uses the tip-diffraction methodology, the ability to electronically steer the sound beam and to display the data in numerous ways gives PA definite advantages over

conventional tip diffraction. For example, it is possible to setup electronic scans that will allow the user to view multiple beam angles from a single scan (Figure 1.2-14). This gives the operator the advantage of finding the optimum angle for detecting a particular crack tip; something that is normally not possible when using conventional tip diffraction. Once the optimum angle is found, the sound beam can then be electronically focused at multiple depths to reduce noise and lessen sizing inaccuracies caused by the effects of beam spread. Additionally, the focusing characteristics can be refined by electronically adjusting the aperture size to select more or fewer elements.

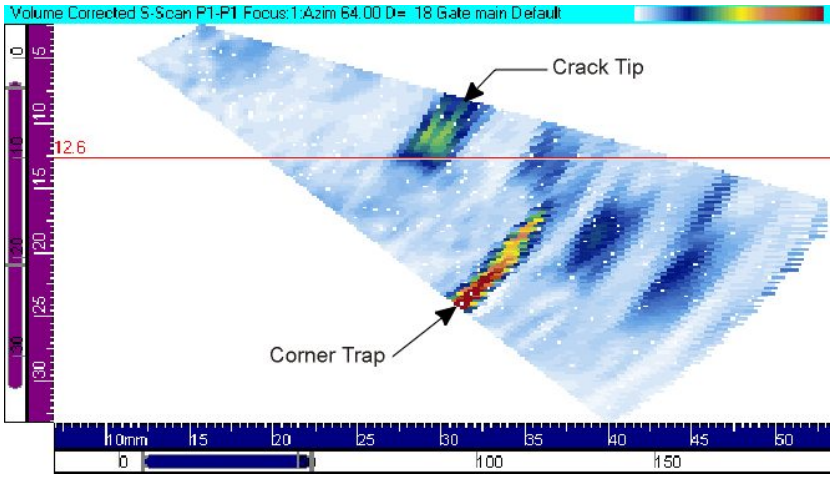

Figure 1.2-14. PA Sector Scan of Crack Tip at Multiple Angles (50 to 75 Degrees)

Tests conducted with PA show that the results obtained with conventional P/E tip diffraction are generally true for PA tip diffraction as well. While direct comparisons to transducer size and frequency could not be made because of physical differences in probe design, optimal beam angles for cracks of various heights were similar. As with conventional tip diffraction, accurate sizing still depends upon the ability to detect and resolve the crack tip. PA, however, has the ability of optimizing the focus and directivity of the sound beam electronically to achieve a good crack tip signal, something that would normally require a large selection of transducers and angled wedges. In fact, with the right probe and wedge combinations, all the other techniques evaluated during this project can be achieved using PA.

Evaluation of TOFD

TOFD is an excellent technique for determining crack size. In fact, TOFD results obtained during this study confirm that the technique provides crack height measurements that are typically more accurate than any of the other techniques evaluated, especially in thicker

materials. However, when properly calibrated, TOFD will usually be more accurate because of the ability to precisely locate and measure the crack tip using software tools.

TOFD has an inherent dead zone near the inspection surface where crack tips may be difficult or impossible to detect. Although the lateral wave will detect the presence of a crack near the inspection surface, the crack tip itself may not be detected. The depth of this near-surface dead zone depends largely upon the beam spread of the transducer, angle of the sound beam, and spacing between the probes.

Although TOFD can provide accurate crack height measurements it can also be very inaccurate if not properly applied. Some of the more important factors affecting TOFD accuracy are listed in the following bullet items:

- Unlike P/E tip-diffraction techniques, TOFD crack height measurements are not linear with respect to the TOFD. As an example, a crack propagating from the back surface that is 25% of the wall thickness in height will appear to be nearly 50% of the wall thickness when compared to the lateral wave and back echo signals (Figure 1.2-15).

- If the crack tip is not positioned exactly midway between the probes, the crack will appear to be deeper than it really is. Consequently, it is necessary to scan perpendicular to the major axis of the crack (B-scan), as well as parallel to the major axis of the crack (D-scan), in order to locate the maximum crack height.

- One critical numerical factor in TOFD calculations is the spacing between the transmitting probe and the receiving probe. If this measurement is not correct, the crack height calculation will be inaccurate. Two common causes of spacing variations are mechanical slop in the probe holder or a change in the exit point of the probes due to wear.

- Depth calculations are normally based on a flat plate having parallel surfaces and uniform thickness. When this is not the case, compensation must be made for variations due to part geometry.

- Variations in the distance between the transducer and the part will also show up in the resulting crack-tip depth calculation. These variations can be caused by changes in the couplant thickness between the probe and the part, or changes in wedge delay caused by wearing away of the wedge. To reduce depth errors caused by inaccurate wedge delay measurements and couplant thickness variations, a relative TOFD measurement between the lateral wave and the tip-diffracted signal can be performed. The depth-to-tip diffracted signal from a crack can then be calculated using the following equation.

$$d = 0.5\sqrt{(C\Delta T)^2 + (4C\Delta TS)} \tag{1-3}$$

where:

d = Depth of crack tip from scanning surface
C = Sound velocity in the material
ΔT = Change in TOFD between lateral wave and crack-tip signal
S = Half the separation distance between the index points of the probes.

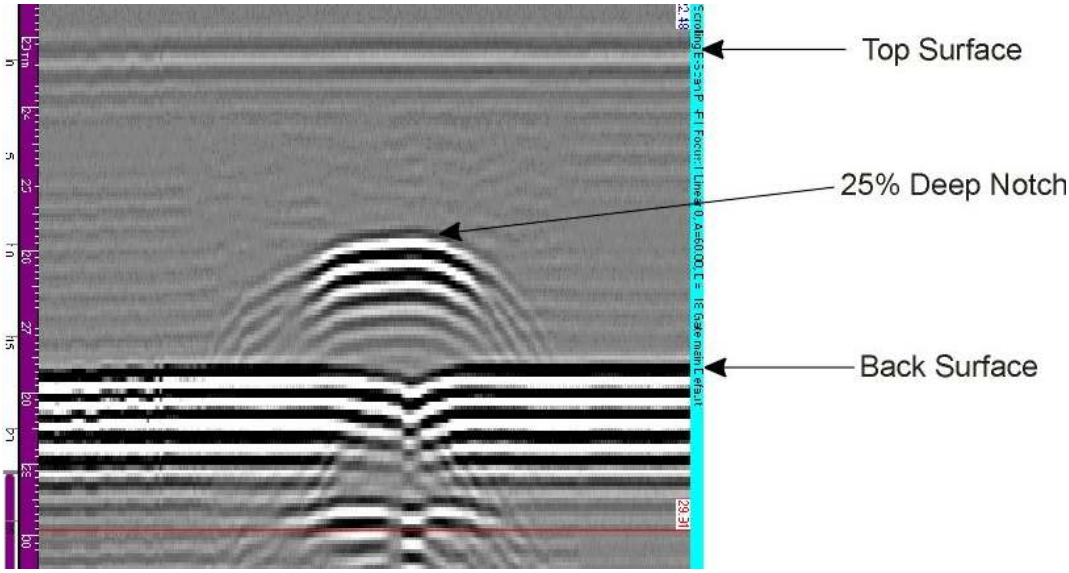

Figure 1.2-15. TOFD B-Scan of 1-in.-Thick Carbon Steel Plate with 25% Deep Notch

Destructive Evaluation of Cracked Samples

During the course of the study, selected samples of each size range were chosen for destructive examination to determine the actual crack height. The purpose of the destructive tests was to compare ultrasonic crack height measurements to actual measurements so that relative estimates of crack sizing accuracy could be obtained.

Thick-Wall Samples [>3 in. (>75 mm)]

Six samples, measuring approximately 35-in. long × 6-in. wide × 6.5-in. thick (889-mm long × 152-mm wide × 165-mm thick), were extracted from the original sections of a thick-wall component. The samples consisted of 5.5- to 6.5-in. (140- to 165-mm-)-thick Cr-Mo steel having a stainless steel weld overlay on the inside surface that measured approximately ½-in.

thick. To simulate cracking that typically occurs in these particular components, a fatigue crack was induced on the stainless steel overlay surface (inner surface) and grown to a specified depth. The goal was to produce crack depths in the range of 0.25 to 2.5 in. (6.35 to 63.5 mm) as measured from the original inner surface. This resulted in the shallower cracks being contained within the stainless steel overlay while the deeper cracks propagated through the overlay-to-base metal interface and into the base metal itself. Length of the cracks varied from less than 2 in. to over 6 in (50 mm to over 150 mm).

The techniques that were evaluated on the thick-wall sections include:

- IDCW
- Manual single-element, P/E tip diffraction (shear wave and refracted longitudinal)
- PA tip diffraction
- Automated TOFD.

The samples used for this evaluation presented some challenging ultrasonic crack-sizing problems. The biggest obstacle was the attenuation of the sound energy within the material due to the combined effects of thickness and small discontinuity indications scattered throughout the base metal and the overlay. Other challenges included refraction and reflection of the sound energy at the overlay-to-base metal interface, irregular surface finish on the outer surface, and curvature of the samples.

For the thick-wall samples, the IDCW technique did not work well; however, the single-element and PA tip diffraction techniques, as well as, the TOFD technique produced good indications of the crack tips. Test results show that the best angle for single-element tip diffraction was approximately 45 degrees. Both shear waves and refracted longitudinal waves worked well for these samples.

The PA P/E tip diffraction results were similar to those obtained using single-element tip diffraction, but the PA allows a larger amount of data to be collected in a single scan on each sample. During the scan of each sample, data was collected at refracted longitudinal angles of 30, 35, 40, and 45 degrees. By scanning at four different angles, the optimum angle for each crack was found. Analysis of the test results show that the crack tips in three of the samples were best detected at a 40-degree angle, two were best detected at 45 degrees and one was detected at 35 degrees. This leads to the conclusion that, for heavy-wall sections, a refracted L-wave angle of 40 to 45 degrees provides the best possibility of detecting crack tips oriented perpendicular to the outer surface.

The automated TOFD technique was evaluated for the thick-wall samples using a refracted longitudinal angle of 45 degrees. For this particular application, TOFD gave good visualization of where cracks were in relation to the inner and outer surfaces, provided the cracks had propagated into the base metal. Cracks in the overlay were difficult to see because of the high noise level at the overlay-to-base metal interface.

Accuracy of the TOFD and P/E tip-diffraction techniques used on the heavy-wall evaluations are shown in Figure 1.2-16. Results indicate that TOFD is the best choice for deep crack sizing for heavy-wall applications. Manual P/E tip diffraction appeared to work well for cracks 1 in. (25 mm) or less in height; however, the technique normally underestimated the height of deeper cracks. This is probably due to failure to accurately detect the crack tip rather than actual measurement errors. Since discontinuities are likely to exist at the overlay interface, these interface discontinuities could easily be mistaken for crack tips, leading to height calculations being obtained from signals other than crack tip signals. In like manner, the corner trap signal and signals from the crack face could also be mistaken for the crack tip.

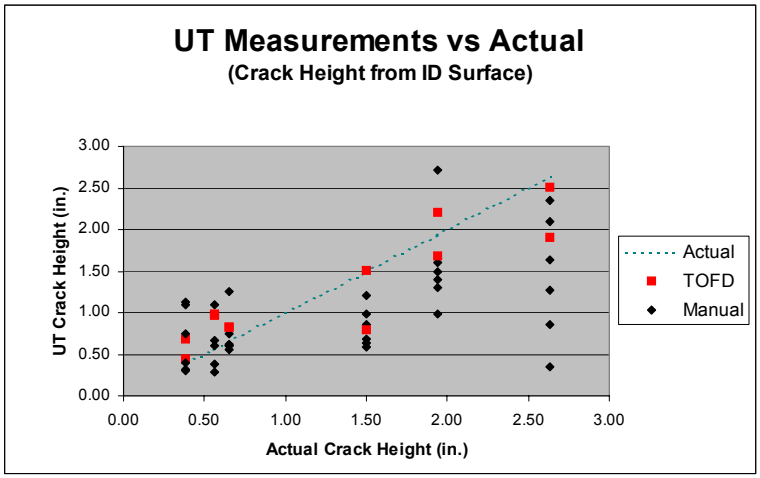

Figure 1.2-16. UT Measurement vs. Actual Height for Thick-Wall Samples

Medium-Thickness Samples [>0.5 and <3 in. (>12.7 and <76.2 mm)]

Samples in this thickness range were fabricated by placing fatigue cracks in A-36, carbon steel base metal, having a 1-in. (25-mm) thickness. By using this thickness, it was possible to compare the accuracy of all five techniques on the same cracks. Table 1.2-1 shows the ultrasonic crack height measurement obtained using each technique, compared to the actual crack height. The cracks were open to the opposite surface and were selected so that two different crack heights could be evaluated. Although the greatest inaccuracy was only 0.048 in. (1.22 mm) (5% of the wall thickness), it must be noted that these measurements were made

under ideal conditions. For actual in-service-type inspections, the inaccuracy of the ultrasonic crack-height measurement is likely to be greater due to factors such as surface waviness, component temperature, and limited transducer access.

A review of data from the five ultrasonic techniques shows that IDCW provided a good estimate of crack height while all the other techniques provided more precise measurements. The dual-element technique worked well on the shallowest crack; however, the deeper crack could not be measured. This was due to the fact that the crack tip of the deeper crack was only 0.32 in. below the top surface and the focal depth of the dual-element transducer was 1 in. The remaining techniques (TOFD, single-element P/E, and PA) all produced similar results with respect to accuracy.

Table 1.2-1. Comparison of UT Accuracy for All Techniques

Crack	Actual Crack Height From Opposite Surface [in. (mm)]	UT Measured Crack Height					Mean Error [in. (mm)]	Std. Deviation [in. (mm)]
		ID Creeping Wave [in. (mm)]	P/E Single Element [in. (mm)]	PA [in. (mm)]	Dual Element [in. (mm)]	TOFD [in. (mm)]		
1	0.349 (8.9)	0.25 to 0.50 (6.4 to 12.7)	0.326 (8.3)	0.337 (8.6)	0.368 (9.4)	0.322 (8.2)	0.020 (0.51)	0.021 (0.53)
2	0.675 (17.2)	0.50 to 0.75 (12.7 to 19.1)	0.669 (17)	0.627 (15.9)	--[(a)]	0.710 (18)	0.030 (0.76)	0.042 (1.1)

(a) Unable to obtain dual-element measurement on deep crack due to focal depth of probe.

Conclusions

It is apparent that no single ultrasonic technique can be used to accurately size cracks. Factors such as crack orientation, crack height, material thickness, and accessibility determine the ultrasonic techniques that can be used.

When using crack-tip diffraction measurements described in this study, signal amplitude is not critical in determining crack height. As long as an adequate tip signal can be resolved, TOF or TOFD measurement can be made.

While some ultrasonic techniques are more accurate for a given part geometry, material type, or crack height, a side-by-side comparison of each technique on medium-thickness samples, indicates that sizing accuracy is similar for all techniques. Regardless of the ultrasonic technique used, accurate crack-height measurements depend upon a combination of four key ingredients:

- Accurate calibration on reference reflectors of known depths
- Detection and resolution of the crack tip
- Accurate TOFD measurement of the sound beam
- An adequately trained and highly skilled operator.

During the course of the study, some techniques were found to perform better than others for certain crack heights. Table 1.2-2 summarizes relative ratings for the ultrasonic techniques used for sizing surface-breaking cracks open to the opposite surface from which the sound beam is entering the part. On pipes these cracks are often referred to as ID-connected cracks. Table 1.2-3 shows similar ratings for cracks open to the surface from which the sound beam is entering the part. These cracks are often referred to as OD-connected cracks.

Table 1.2-2. Relative Ratings of Ultrasonic Sizing Techniques for ID-Connected Cracks

Thickness Range	Suspected Crack Height[(a)]	ID Creeping Wave	P/E Tip Diffraction						TOFD	Dual Element
			Shear Wave			Refracted L-Wave				
			45	60	70	45	60	70		
< 0.5 in. (< 12.7 mm)	< 25%	●		■						
	25% to 50%	●		●	■					
	50% to 75%	X		●	■					
0.5 to 3.0 in. (12.7 to 76.2 mm)	< 25%	X	●	●					■	●
	25% to 50%	X	●	●	●				■	●
	50% to 75%	X		●	●				■	X
3.0 to 7.0 in. (12.7 to 178 mm)	< 25%		●			●			■	
	25% to 50%		●	X		●			■	
	50% to 75%		●	X		●	X		■	

(a) Note: Crack tips less than 5% to 10% of wall thickness may not be adequately resolved.

Best ■ Good ● Fair **X**

Table 1.2-3. Relative Ratings of Ultrasonic Sizing Techniques for OD-Connected Cracks

Thickness Range	Suspected Crack Height[(a)]	ID Creeping Wave	P/E Tip Diffraction						TOFD	Dual Element
			Shear Wave			Refracted L-Wave				
			45	60	70	45	60	70		
< 0.5 in. (< 12.7 mm)	< 25%			■	X					
	25% to 50%			●	■					
	50% to 75%	●	X	●	■					
0.5 to 3.0 in. (12.7 to 76.2 mm)	< 25%			●	■					
	25% to 50%			●	●				■	X
	50% to 75%	X	X	●	●				■	X
3.0 to 7.0 in. (12.7 to 178 mm)	< 25%				●			X	■	
	25% to 50%		X	●	X		X	X	■	X
	50% to 75%		X	●		X	X		■	X

(a) Note: Crack tips less than 5% to 10% of wall thickness may not be adequately resolved.

Best ■ Good ● Fair **X**

Study 4 – Validation of AUT Sizing Accuracy[1.2-1]

General

The study performed at EWI was focused on girth weld discontinuity sizing, as measured by mechanized UT using the P/E and TOFD as well as PA ultrasonic technology.[1.2-1] Incomplete fusion type of defects were manufactured in girth welds with a CRC-modified 5-degree J-bevel weld configuration of 914-mm (36-in.)-diameter, 14.9-mm (0.562-in.)-thick API X70 pipe welded using automatic GMAW. Significant change from normal welding parameters was carried out to induce the defects in welds. Twenty-four sidewall LOF and six transverse inter-run LOF or cold laps were developed. EWI performed in-house flaw verification using digital radiography and PA technology at ambient temperature. Digital radiography validated the location and length of each flaw. Less than 60% of the flaws were detected by radiography. The PA detection and sizing technique and imaging software were used to validate the location, length, and depth of each flaw. The flaw height was measured by time-based, tip-diffraction techniques using a single transducer (single crystal or PA probe). In addition to the typical A-scan tip-diffraction presentation, a combination of B- and C-scans and non-corrected/corrected sectorial (S-) scan imaging techniques were applied for better data visualization, interpretation, and depth/length measurements.

AUT Approaches and Trials

Several blind mechanized UT trials for sizing of girth weld defects using the zonal concept, P/E, and TOFD methods and PA technology were conducted with various AUT vendors. Each AUT contractor fabricated its own calibration block according to the requirements of ASTM 1961-98.

A summary of AUT approaches used for the trials is shown below:

- Zonal discrimination with focused P/E multi-probe
    - Optimization of beam profile through variation of radius of curvature (lenses or curved element), element size, and frequency
    - Optimization of sizing through amplitude linearization (Approach A1)
    - Optimization of sizing through proprietary defect-sizing algorithms (Approach A2).

- Zonal discrimination with non-focused pulse-echo multi-probe (Approach A3)
    - Optimization of beam profile of flat probes through variation of element size and frequency

- Optimization of sizing through amplitude adjustment and determination of signal signature or echo dynamic
- Optimization of sizing through zone interaction rules.

- Zonal discrimination with focused P/E PA probes
  - Optimization of beam profile through focal laws, element size, and frequency (Approaches A4, A5, and A6; 7.5-MHz, 48-element linear PA probe for Approach A4; 7.5-MHz, 64-element linear PA probe for Approaches A5 and A6; 10-MHz, 32-elements linear PA probe for Approach A6A)
  - Optimization of sizing through amplitude linearization (Approaches A4 and A5)
  - Optimization of sizing through sectorial scanning and tip-diffraction measurements (Approaches A6 and A6A – under development).

- TOFD is added to all approaches for supplemental defect information, improved characterization, and sizing.

- A1 to A5 are amplitude-based sizing approaches.

- A6 and TOFD are time-based sizing approaches.

The blind tests were conducted at vendors' laboratories. No accept/reject criteria were applied and all indications considered significant were reported. Each crew performed nine scans on each weld. Three scans were at the proper guiding band position, three scans were at +0.5 mm (0.02 in.) from the proper guiding band position and three scans were at -0.5 mm (0.02 in.) from the proper guiding band position. At the end of the blind test each vendor provided an electronic and hard copy of the summary report form for each.

Destructive examination for verification of blind and open-trial NDT results and evaluation of the real size and location of the defects was performed. ID and OD notches (secondary cuts) were machined in each plate opposite to each flaw. A failure in the desired location was initiated after cooling the wide plate in liquid nitrogen and performing 3-point bend loading of the plate to expose up- and downstream flaw surfaces. An example of exposed up- and downstream LOF surfaces is shown at the bottom of Figure 1.2-17. The height of each flaw was measure with 0.5-mm (0.02-in.) increments on each surface. The same step of increments was used for sectioning (machining) of several LOF that we were not able to expose. The length of each LOF was measured on each exposed fracture surface. The average fractographic and metallographic results for the height of 24 LOF depicts average of 10 data points in the highest part of the flaw, as defined by destructive measurements. The destructive results reveals that the average height of two flaws is less than 1 mm (0.04 in.), the average height of four flaws is in the range of 1 to 2 mm (0.04 to 0.08 in.), the average height of 14 flaws is in the range of 2 to

4 mm (0.08 to 0.16 in.), and the average height of four flaws is larger than 4 mm (0.16 in.). A typical standard deviation of the actual measured height is less than 0.5 mm (0.02 in.)

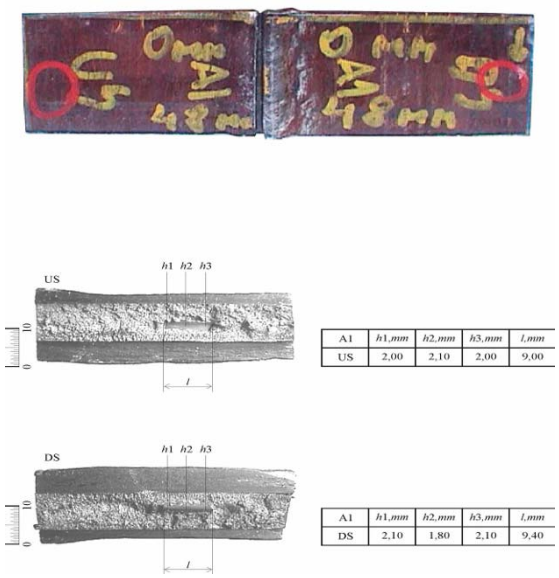

A1	h1,mm	h2,mm	h3,mm	l,mm
US	2,00	2,10	2,00	9,00

A1	h1,mm	h2,mm	h3,mm	l,mm
DS	2,10	1,80	2,10	9,40

Figure 1.2-17. Destructive Flaw Validation – Wide Plate and an Exposed Flaw

Statistical Analysis

Statistical analysis and graphical presentation of the destructive and NDT results were performed. Six transverse flaws were excluded from the analysis because AUT vendors were not prepared for reliable detection of this type of flaws. Only the results for a total of 24 sidewall LOF flaws were analyzed.

The statistical analysis focused primarily on determining the average maximum flaw height error since the height of the flaw is the most critical parameter for engineering critical assessment (ECA)-based assessment. A comparison between the measured UT height and the actual maximum average height is presented in Figure 1.2-18 for each approach. A significant scattering was observed for the results obtained using Approaches A1, A4, and A5. The results obtained using these approaches show undersizing of LOF when the height of the flaw is in the range of 4 mm (0.16 in.). Good correlation is achieved using Approach A2. Only one case for undersizing below 95% limit against undersizing is observed for Approach A2. In several cases oversizing for Approach A2 is a significant. The population of results reported using Approach A6 is very small and no trends were observed. At the same time, the results of the open trial using PA technology (Approach A6A) are very encouraging.

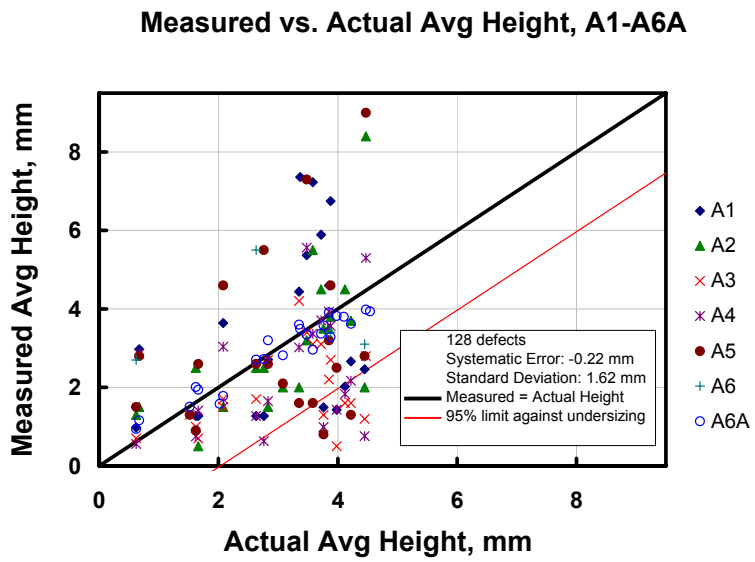

Figure 1.2-18. Measured vs. Actual Average Height – Approaches A1-A6 and A6A

Some of the reported TOFD results were used to calculate the height average error for TOFD method as a separate technique. The accuracy shown in Figure 1.2-19 is below the accuracy reported for TOFD in the open literature. Probably, the use of TOFD for girth weld inspection as a separate, independent method will be very risky.

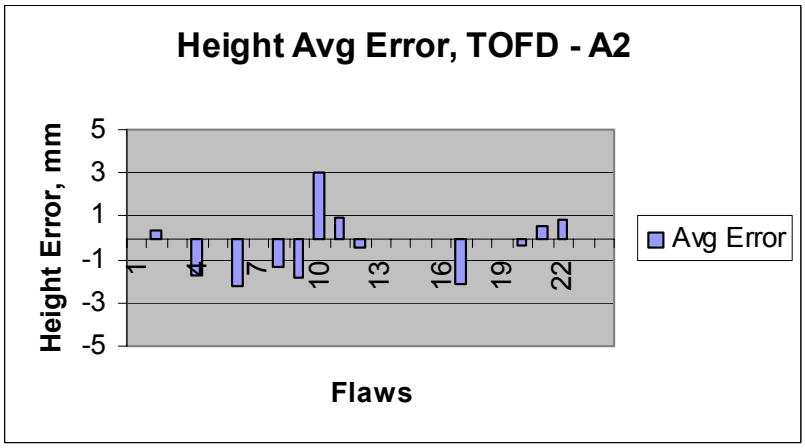

Figure 1.2-19. Height Average Error – TOFD

Only one vendor observed and reported differences in height and length measurements between the multiple scans and/or variable band positions within ±0.5 mm (±0.02 in.). A typical value for the standard deviation is less than 0.5 mm (0.2 in.). Multiple scans and/or variable band positions within ±0.5 mm (±0.02 in.) did not significantly affect the accuracy of flaw sizing. The average error in the estimations for the flaw depth was in the range of -2 to +7 mm (-0.08 to +0.28 in.). The results are shown in Figure 1.2-20 for Approaches A1-A6. Depth depicts average of 10 distance data points from the scanning surface to the top extreme of the flaw in the highest part of the flaw, as defined by destructive measurements. The depth error is related to height error and the similar tendency in depth error was examined.

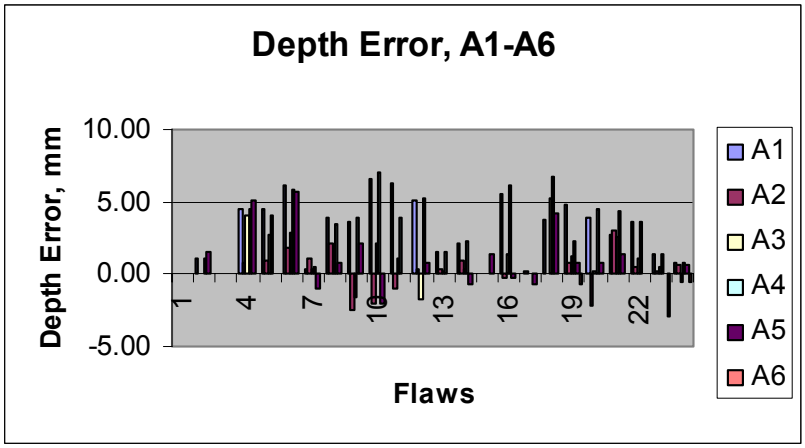

Figure 1.2-20. Depth Average Error – Approaches A1-A6

All vendors were able to determine the flaw length within ±10 mm (±0.4 in.) with several real exceptions. The results are summarized for the Approaches A1-A6 and shown in Figure 1.2-21. The accuracy of the PA approach can be improved by reducing the focal spot size in a plane parallel to the scanning direction. A typical sizing accuracy for lengths within ±5 mm (±0.2 in.) was achieved using a PA transducer with a small spot size.

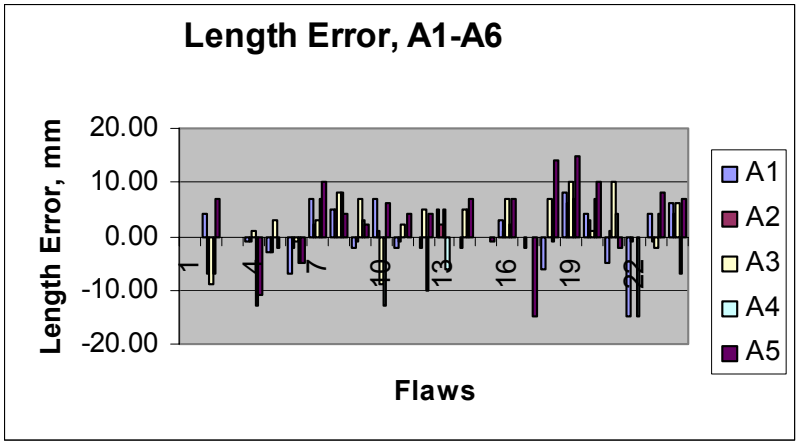

Figure 1.2-21. Length Average Error – Approaches A1-A6

Table 1.2-4 summarizes the realistic expectation for sizing accuracy uncertainties that can be incorporated into probabilistic assessments and reliability-based acceptance criteria documents. In the best case only 45% of the flaw population will be sized within ±0.5-mm (±0.02-in.) accuracy. The majority of the defects will be sized within ±2-mm (±0.08 in.) accuracy.

Table 1.2-4. Achieved Height Sizing Accuracy

Acronym	Approach Description	Height Sizing Accuracy, Avg. Error "a" in mm (in.) and % of Detected Flaws		
		a< ±0.5 (0.02)	±0.5 (0.02) >a< ±2 (0.08)	±2 (0.08) >a< ±4 (0.16)
A1 - blind	Focused multi-probe, amplitude linearization	35	35	30
A2 - blind	Focused multi-probe, proprietary sizing algorithm	45	45	10
A3 - blind	Non-focused multi-probe, zone and amplitude interaction rules	30	45	25
A4 - blind	Focused PA, 48 el., amplitude linearization	40	20	40
A5 - blind	Focused PA, 64 el., amplitude linearization	15	35	50
A6 - blind	Focused PA, 64 el., sectorial scanning	25	25	50
A6 -open	Focused PA, 32 el., raster and sectorial scanning	75	25%	n/a

Conclusions

The best accuracy was achieved using shaped focused multi-probes with sizing algorithms. When using non-focused multi-probes, the flaw height was typically undersized. PA technology demonstrated superior sizing accuracy at the open trial but was below the expected level of accuracy at the blind trials. In the best case, only 45% of the flaw population will be sized within ±0.5-mm (±0.02-in.) accuracy. The majority of the defects will be sized within ±2-mm (±0.08-in.) accuracy.

As it is stated at the start of this section the performance of AUT systems for a particular use is based on number of variables which can be seen from the above mentioned studies. There are number of variables that plays important role in the AUT performance. Better definition is required to understand the capabilities of each system and select the best for a specific use on the project. There needs to be a study performed on various variables and its effect on the AUT results and share the information in the industry, based on information gathered, lessons learned the AUT companies can improve in order to meet the targets and thus benefits the industry overall.

Study 5 – Review of Defect Sizing in Pipeline Welds[1.2-21]

The popularity of "fitness-for-service" (FFS) acceptance criteria is gaining more acceptance now because of fracture mechanics. Fracture mechanics based on material toughness and crack growth data leads to initial defect size. The AUT sizing error is then build into the initial defect size to give the final acceptance criteria. This states that the sizing accuracy of AUT system plays a very important role. There have been many pipeline sizing studies performed in last few years that we reviewed and are summarized as follows by Moles[1.2-21].

Battelle PNL Study

This study consisted of using seven teams to perform inspection concentrated on nuclear pipeline detection.[1.2-22] This study consisted of various aspects like materials, real defects, etc. The results showed that pipeline defect sizing was poor, with major sizing errors.

University of Ghent Studies

This study was sponsored by the International Pipeline and Offshore Contractors Association (IPLOCA) and centered on detection and sizing.[1.2-23] Both AUT crews found detection to be good; sizing produced a standard deviation of defect sizing to within ±1.5 to 2 mm for surface-breaking defects.

Transco Trials

A study was performed by Advantica for GTI with seven inspection companies for detecting approximately 90 typical implanted defects like porosity, LOF, copper cracking, and transverse defects. The aim of the program was defect detection, the defect sizing varied from 1.1 to 1.8 mm.[1.2-24,1.2-25] More details about Transco trials are described in the Study 6 section.

Shell Results

This internal study contains data collected from several programs[1.2-26] and shows considerable scatter within the ±1-mm eyeball range. There is a paper based on several programs that refers to sizing accuracies of ±0.3 mm (not defined in the paper; however, it assumed absolute error not standard deviation).

Saipem Study

The results of the study performed revealed little undersizing or oversizing.[1.2-27] The author found out the range of ±1-mm on sizing. The study also shows the comparison of conventional multi-probe and PA AUT systems and found that when using the same setup the differences were negligible as predicted by physics.

Oceaneering OIS Qualification

This Oceaneering study produced a noticeably lower standard deviation of $\sigma \sim 0.6$ mm.[1.2-21] The data set contained mostly sidewall LOF. It was concluded that PA offers significant sizing advantages and better results were achieved by using this system.

EWI Round Robin

The project described in the previous section used two pipes containing effectively 24 LOF defects and the results revealed considerable variance even when using identical procedures.[1.2-1] In the best case, 45% of the defects were sized within ±0.5 mm and the majority within ±2 mm. EWI was able to inspect the defects to an accuracy of ±0.6 mm with multiple techniques on the inspection.

Det Norske Veritas

Studies by DNV on defect sizing using one amplitude-based and one TOFD-based data set showed a typically low standard deviation σ.[1.2-19] Undersizing was minimal, and the systematic error was small in both cases (~0.1 mm). The standard deviation was ±0.41 for one data set and ±0.62 for other set which is a significantly lower error. Examples of DNV sizing results are shown in Figure 1.2-22.

R/D Tech Data

The R/D Tech data studied revealed limited undersizing, some significant oversizing, and low mean sizing error.[1.2-21] Calculation of sizing accuracy using the ASME approach gave an RMS value of over ±1.1 to 1.7 mm depending on the data set used.

Conclusions

The conclusions drawn from the studies above were that consistent results were achieved with the use of different processes. The trend shows a trend toward oversizing, not undersizing for small defects. Mean sizing error was found typically below 1 mm, with a random sizing error. Studies also show the sizing errors falling within an eyeball range of ±1 mm and standard deviation σ varies up to ±2 mm depending on defects nature and size.

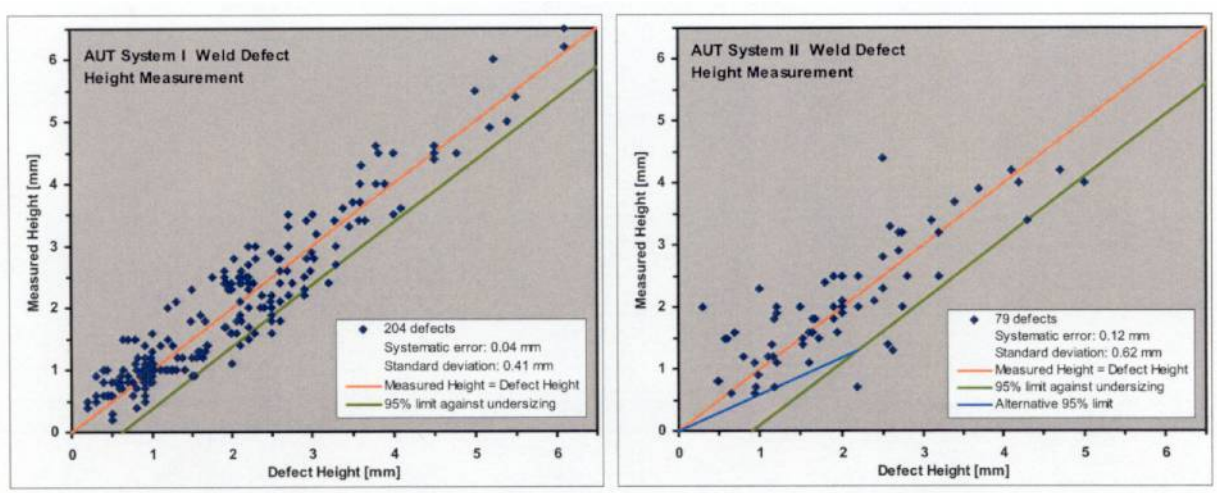

Figure 1.2-22. **Examples of Defect Height Sizing Errors and Limits Against Undersizing** (Courtesy of DNV)

Study 6 – Performance of AUT on Mechanized Pipeline Girth Welds[1.2-24,1.2-25]

Nine butt welds were fabricated in 48-in. (1220-mm) diameter, X80 grade, pipes using two mechanized welding systems.[1.2-24,1.2-25] These welds contained a range of deliberately made defects. Seven AUT contracting companies were invited to bring their equipment to inspect the welds at a Transco site and report on the defects they found. Each company inspected the welds independently. The objective was to establish the effectiveness of AUT as an adequate alternative to radiography for pipeline construction when using mechanized welding.

Weld Defects

A wide range of defect types and condition was specified for specialized welding contractors to insert into the welds during their fabrication. The resultant welds were inspected using panoramic X radiography. They were also radiographed again and digitized both for the record and as an additional check. The distribution of the types of defect that were produced is illustrated in the table of Figure 1.2-23. A plot of the RT lengths of the defects, also shown in Figure 1.2-23, demonstrates that they were deliberately made to be short and so they were more difficult to detect with AUT.

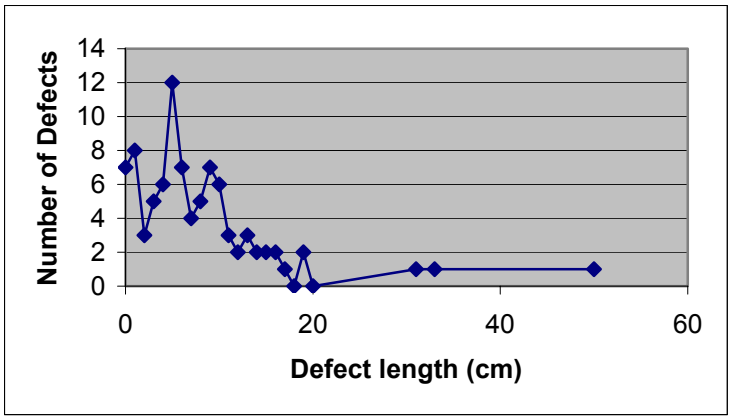

Type of Defect	No.
Porosity	15
LOF	44
Lack of Root Fusion/Pen.	17
Transverse	7
Other	14

Figure 1.2-23. Distribution of Length and Types of Defect Included in the Tests

Results

The results confirmed that very good detection performance is generically available from AUT systems. All linear features longer than 10 mm were detected by some of the systems tested, as well as, most clusters of porosity above 10 mm. Overall, the LOF and lack-of-root-fusion defects were detected in 94 and 90% of the cases, while porosity was detected only 75% of the time. The transverse defects were detected only in about 70% of the cases. Scattered or isolated features, including pores, cavities, and inclusions (metallic and non-metallic), were generally not detected. Neither were geometric features, such as "low cap", "underflush" or "flush root" reported.

AUT is generally considered better than RT in detecting planar defects and this was confirmed by these results. The start of a defective area was shown to be detected earlier by the AUT in many of the defects that were sectioned (e.g., Figure 1.2-24 indicates that a lack of side wall fusion of even 0.5 mm through-wall height has been detected).

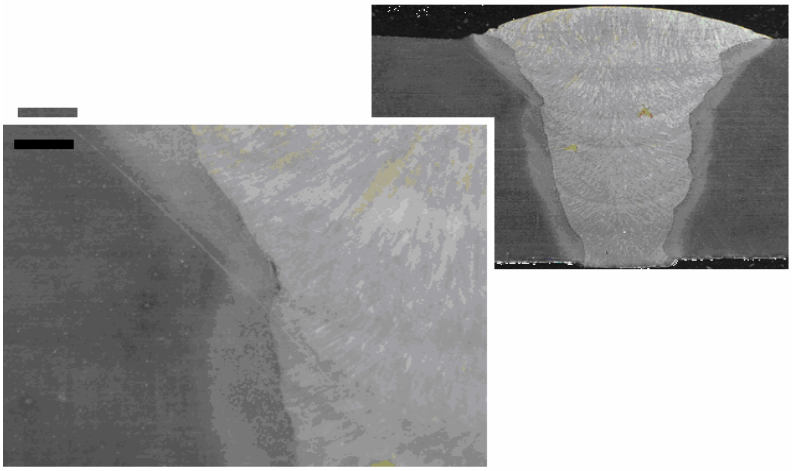

Figure 1.2-24. **The LOF Defect on the Left Fusion Face, at 5 mm from the Outer Surface, was Found by all but One AUT System** (It was not visible at all on the radiographs. Wall thickness = 16 mm, 1-mm bar on enlargement.)

Some variation between inspection companies was apparent, indicating a lack of consistency. This is illustrated in Table 1.2-5.

Table 1.2-5. Breakdown of Missed Defects

Defect Type	Missed by 1 or More Inspections (%)	Missed by 2 or More Inspections (%)	Missed by 3 or More Inspections (%)	Missed by 4 or More Inspections (%)
Porosity	58	41	41	25
LOF	38	23	13	8
LOF Fusion/Penetration	46	40	27	13
Transverse	100	60	40	20
Other	88	75	62	50

While porosity is confirmed as problematic for defection, it is worth noting that half of the inspections found 75% of these small areas of porosity.

The transverse defects were not detected well, especially the external slots.

The “other” defects which are not good ultrasonic reflectors include geometric features (such as low cap, underflush, or flush root) and account for the low detection rate.

The human operator’s individual interpretation of the data is an important factor when the complexity of the data is considered. In order to get good performance in field operations with AUT systems, this suggests that attention to the competence of the operator is essential. An on-the-job test of operator competence has been proposed for Transco operations, as is done for welders.

Three of the eight inspections were conducted using PA equipment. No trend was evident to suggest that either better or worse results were obtained with the PAs.

When considering the deficiencies of AUT, one should remember that RT is by no means a perfect inspection method to compare it with. However, in comparison the approach does allow a good breadth of coverage.

<u>The Detection of Copper</u>

Several areas of copper, inserted into the weld, were available for study. No pick up of copper from the internal backing plate was evident.

The most easily detected area (called "craze cracks" by RT) was detected by all the AUT systems, but was generally characterized as "porosity". A section (Figure 1.2-25) shows this form of cracking to be much like liquation cracking and is distributed throughout the weld so that its misclassification as porosity is understandable.

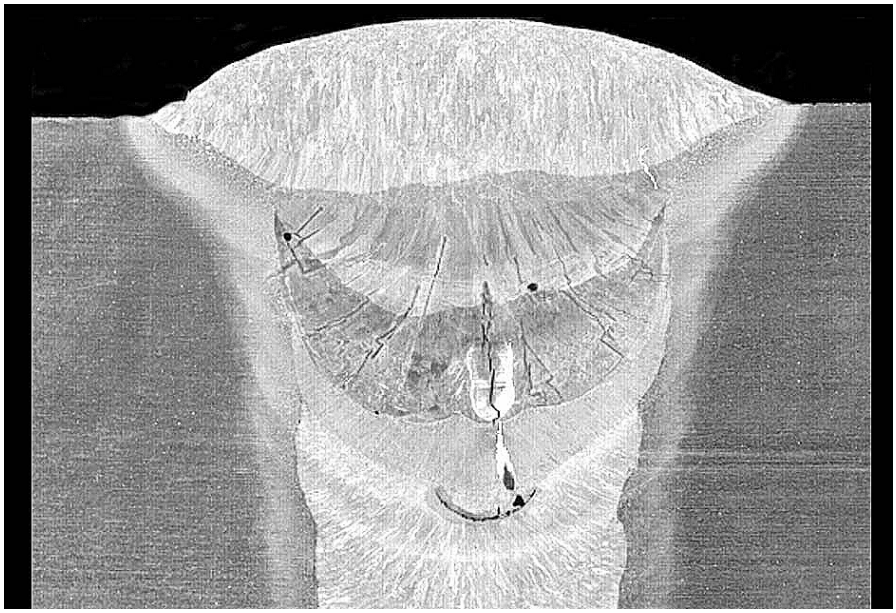

Figure 1.2-25. Defects Associated with Copper in the Weld

The second area of copper was only detected by RT as a small "transverse defect"; most of the feature was invisible on the radiographs, even on careful re-interpretation. When it was sectioned, it proved to be more complex than expected and extended along the weld length (>12 mm). Only one company detected it as a transverse feature, though two others also reported a "planar" element. Generally, it was reported as porosity. The second area of copper induced cracking has unique transverse defects that caused some complications in AUT detection and defect characterization.

Transverse Defects

The transverse slots that were cut across the welds were generally detectable, but with some notable "misses". Each of the internal slots was eventually detected across the board (one company did so only on a second attempt). The detection of the external slots was more variable. About half the AUT companies missed the external slot in the J-prep weld but only two missed that in the CRC-type weld.

It has to be noted that the calibration block are machined and has no replication of the root or cap. It might worthwhile to consider the application of false cap with the calibration block to reduce timing errors.

The detection of these defects is not covered in standards and an industry initiative to improve this aspect may be warranted.

Seam Weld Region Defects

It is very important to consider the AUT inspection at the area of the long seam weld. The ultrasonic properties of the seam weld material are unknown, so it cannot be assumed that the ultrasonic beams are appropriately targeted. It would be recommended, any defect that extends into such an area might need to be further examined manually. Alternatively, such a defect could be assessed with an additional length added equal to the width of the pipe seam weld (i.e., assume that the defect extends right across the seam weld area). This aspect of inspection needs some special attention by the AUT industry because no formal studies to address the seam weld region defects are available. Typically tracking of long seam defects is performed at steel mills.

Size Measurement

The main aspect of size measurements are height and length of indication. The length measurement tends to be generally longer than actual when inspected ultrasonically, while the height measurement has always been difficult has produced varying errors. The use of TOFD has aided the height measurement to certain extent but it has to be kept in mind that the TOFD has limitations on the indications that are near surface. As discussed in previous sections, different systems tend to perform in different manner as far as sizing of indication is considered. There are so many variables that plays very important role during sizing and if right tools are used the error on sizing can be reduced.

An improved method, using the special options of PA data, has been demonstrated on calibration defects. An accuracy of better than 1 mm has been cited but it is unlikely to be as good for real defects.

When defect size values are put into ECA assessments a substantial conservatism becomes apparent. There is a need to study more on the complexity of the AUT sizing for various kinds of defects and a method to accommodate it during ECA. The consideration is required on both sides of the AUT system, procedure, and operator and ECA analysis to narrow down the conservatism.

Conclusions

The AUT systems on trial have produced inspection results that compare well with radiography, with good detection except for isolated pores and inclusions. Clustered porosity is frequently found, especially larger clusters. Copper cracking is generally misclassified when it is detected and so may be left un-repaired. Transverse defects are not detected reliably with the current transverse probes arrangement and needs some improvements.

Study 7 – TOFD Enhancement[1.2-28]

TOFD is being used more and more in mechanized UT systems. The use of TOFD has lots of advantage but not if used as stand-alone technique. TOFD provides a safety net for inspection of some critical defects. Limitations of TOFD can be stated as mentioned below:

- Poor detection/sizing near the entry surface
- Requires a second axis of motion to define the side of a weld
- Optimum probe centre spacing can result in probe interference with weld cap
- Mismatch conditions (misalignment-ID/OD) mask root defects in back wall signal.

However, when TOFD used in combination of standard P/E method provides very useful information and it is observed that the two techniques compliment each other.

The typical defect found in welds made using automatic welding is LOF on the bevel sidewalls and for manual welding the most common defects are slag, hollow bead, and porosity.

Table 1.2-6 indicates some of the more common indications and the weld process they are associated with. Table 1.2-6 also indicates approximate detection capabilities with the various NDT methods used in pipeline weld inspections. Unfortunately, no references were shown in this study to support so-called POD data in the table.

The authors performed study of each presentation formats (TOFD, B-scan/mapped data, and amplitude-TOF strip charts) and some of findings are as follows:

- Defects like porosity in manual welds is easily seen on TOFD but not notable on P/E strip chart.

- TOFD can see slag but cannot be sure how close to surface.

- Crack seen with both TOFD and P/E irregular travel time on P/E and loss of back wall signal in TOFD indicates the ID surface breaking. Based on amplitude exceeding a threshold over a minimum length this defect could be acceptable without TOFD information to aid in evaluation.

To conclude:

- Strip chart (peak amplitude and TOF) scores low on hollow bead, small porosity, unacceptable mismatch, and burnthrough.

- Raw data (B-scans or mapping) scores low on hollow bead, small porosity, unacceptable mismatch, and burnthrough.
- TOFD scores low on transverse cracks and defects near the OD surface.
- X radiography scores low on planar defects.
- So a combination of all above methods will give the best POD but economically not possible. The best compromise is obtained from mechanized ultrasonics where P/E and TOFD are used in combination.

Table 1.2-6. Summary of Performance of Different Techniques

Imperfection	Mechanized Welding	Manual Welding	POD X-ray (%)	POD Pulse Echo (Map) (%)	POD Strip Chart (TOF and Amplitude) (%)	POD TOFD (%)
LOF surface	Yes	Yes	90	95	95	OD 0 ID 60
LOF subsurface	Yes	Yes	50	100	100	100
LOF interpass	Yes	Yes	0	50	30	100
Slag	No	Yes	100	90	90	100
Porosity (>5%)	Yes	Yes	100	95	50	95
Undercut	Yes	Yes	100	90	90	ID50 OD 0
Misfire	Yes	No	100	100	100	55
Lack of cross penetration	Yes	Yes	90	75	75	100
Incomplete penetration	No	Yes	100	100	100	75
Hollow bead	No	Yes	100	25	25	0
Centerline crack	Yes	No	75	75	75	100
Under-bead crack	No	Yes	60	100	100	100
Transverse crack	No	Yes	75	75	75	0
Mismatch (high-low)	Yes	Yes	60	10	10	100
Root bead misalignment	Yes	No	50	100	100	50
Burnthrough	Yes	Yes	100	50	30	100

Notes:

1. Defects detected with X ray do not reveal depth position or vertical extent
2. Defects detected with UT are compared to calibration reflectors and, therefore, through-wall thickness dimensions and position.
3. Percentages given are not intended to be exact values but merely estimates to show the POD due to the physical limitations of various methods.

1.2.2.3 AUT Advancements

Study 8 – Wall Thickness Compensation for Seamless Pipe Inspection Using PAs[1.2-29]

The problems associated with AUT inspection of seamless pipe are very well known. The main cause for these problems is wall thickness variation of seamless pipes. Lately, there have been few projects that have been executed that have shown a very complex methodology to be followed to overcome the problems with inspection of seamless pipes.

Wall thickness variation on seamless pipe can vary up to 12.5% of the nominal wall thickness. Using standard AUT girth weld inspection techniques like zone discrimination girth weld inspection techniques can totally miss defects if the actual pipe wall varies significantly from the calibration block.

In order to overcome the issues with wall thickness variations a study was performed which consisted of testing with two methods:

- The first method used was to use two calibration blocks; one calibration block to represent the maximum wall thickness and another calibration block to represent minimum wall thickness. Based on these two calibration blocks two sets of focal laws were created and the pipe were scanned.

- The second method to use the two focal laws as mentioned above to interpolate a third group of focal laws that represents intermediate wall thickness. The pipe was scanned with all three setups.

The experiment consisted of manufacturing calibration blocks with maximum wall thickness (H-block), minimum wall thickness (L-block) and median wall thickness (M-block). The results were compared by inspection of the test block with median wall thickness. The AUT setup also consisted of capabilities of wall thickness measurement by generating normal beam.

The main four focal law groups used in the setup based on above mentioned description is as follows:

- For maximum wall thickness (H-channel)
- For minimum wall thickness (L-channel)
- For median wall thickness (M-channel)
- For thickness variation measurement.

H-channel was calibrated using H-block, L-channel was calibrated using L-block, and M-channel obtained from interpolation with the H- and L-channels. The performance of this was checked with use of M-block.

Experiments showed that calibrated L-channels did not inspect the H-block satisfactorily and vice versa, thus enabling to conclude that only one calibration block setup is inadequate for use in cases of wall thickness variations.

While the setup that used H-, L-, and M-channels showed that if the test block is scanned directly with H- and L-setups there would be some targets missed but the interpolated M-channel inspected the block quite well and not missing any targets.

The data offers new method for inspecting seamless pipe with wall thickness variations with a disadvantage of usage of multiple channels that might affect the data transfer rate and thus slow down inspection.

Study 9 – Advances in Imaging of NDT Results[1.2-30]

General

This study explains a new inspection method that is based on method used in the field of seismic exploration of the subsurface of the earth or ocean.[1.2-30] The principle for seismic exploration is based on measurements of echoes caused by acoustic reflection from layers in the subsurface. Generated acoustic signals at the subsurface are recorded by array of microphones. With this data and basic wave theory [inverse wave field extrapolation (IWEX)], a reconstruction of the layers in the subsurface can result in an image. Principles of creating an image using IWEX are described below.

In this technique the elements for the imaging process are used without time delays which are different than what done in PA where a beam is generated by firing adjacent elements with a given time delay. In this technique a data set is created by firing from one element and receiving the response on all the available elements. The data can be stored in a three-dimensional matrix; the three coordinates being: transmitter, receivers, and recorded time base (see Figure 1.2-26). The data matrix in this case contains all possible information as all available transmitters and receivers are used. The A-scan in the data matrix corresponding to the used elements is time shifted and added after the measurement is done. In this technique of IWEX imaging A-scans can be used again for other time shifts corresponding to other beam angles and focal spots. The quality of image in this case is dependent on the number of transmitters and receivers, area covered by the transmitters and receivers, and band width of the signals received. All above parameters requires to be optimized for achieving the best results.

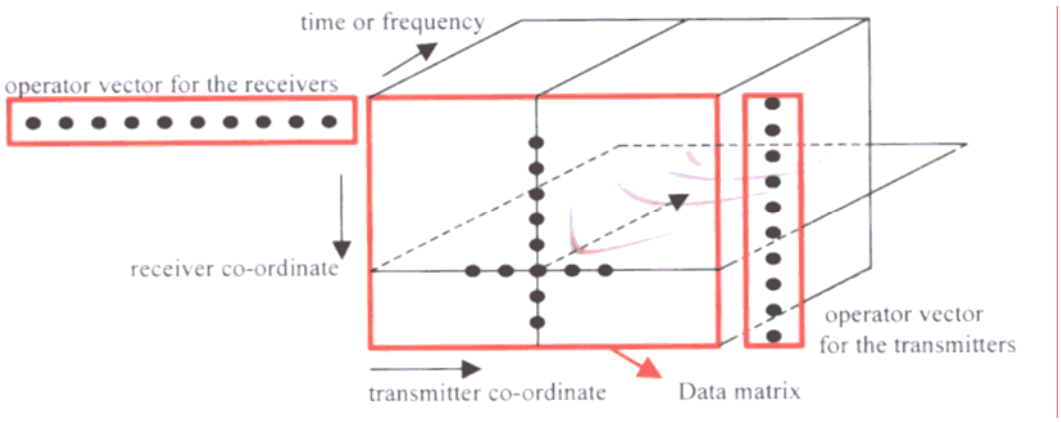

Figure 1.2-26. **3D Data Matrix for all Transmitter and Receiver Combinations** (The vectors V_s and V_r operate on a slice of the data matrix.) (Courtesy of RTD)

Imaging

The four commonly used imaging techniques in this study are:

- Sector scans
- TOFD
- MultiSAFT
- Strip charts.

- **Sector Scans:** Sector scans are obtained by steering beam in small increments as shown in Figure 1.2-27. The result of this scan is presentation of cross section of the weld volume as seen in medical applications. The important fact about the use of this type of scan is that not all indications can be seen in this scan. Some planar defects based on their orientation can reflect in such a direction that they do not show up in the scan. In addition, not all positions in the volume are covered, thus not all directions and beam positions are incorporated in sector scans.

- **TOFD:** A TOFD scan is obtained with two single-element transducers with a large beam width placed on either of weld (pitch-catch method). Based on arrival times of different events a scan is built up in this case. Figure 1.2-28 describes various events covered by the TOFD scan. The defect is observed as disturbance between first signal caused by lateral wave running just under the surface and reflection of the back wall. A TOFD image is less dependent on defects orientation. Because this view is 2D side view picture of a 3D scanned volume it is difficult to know the defect location in the weld cross section.

- **SAFT:** A SAFT image is obtained by placing two single-element transducers, a transmitter and a receiver, both on same side of weld (tandem setup). A-scans are obtained by varying the position of transmitter receiver combination along with the aperture and data is stored in to the data matrix. The image is achieved after processing (Figure 1.2-29) which is a focusing method, compensating only the travel time of the first arrived signals for each point of inspection volume. MultiSAFT takes more possible arrival times into account; however, no amplitude corrections or signals caused by mode conversion are taken into account for both SAFT and MultiSAFT.

- **Strip Chart:** A strip chart is mostly used in girth weld inspection with zonal approach. The cross section of weld is divided into several zones based on the wall thickness. Each zone is inspected from either side of the weld with an ultrasonic beam aimed perpendicular to the weld preparation. The information of a single strip represents the amplitude and transit distance in a time gate corresponding to the position of the expected signal. The defect will appear in the time gate as shown in Figure 1.2-30. The amplitude is calibrated by the use of known reflector.

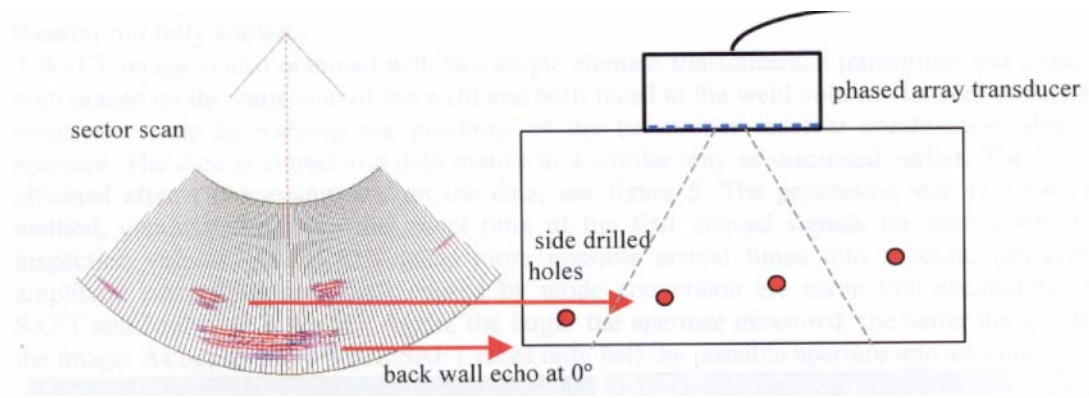

Figure 1.2-27. **Sector Scan made on a Block with SDH** (Courtesy of RTD)

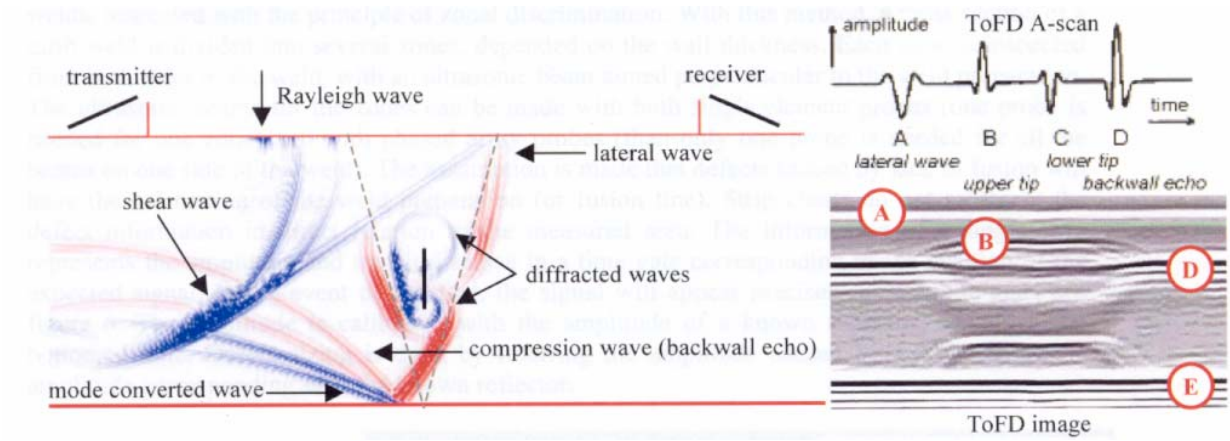

Figure 1.2-28. **Elastic Finite Difference Simulation of the TOFD Principle, Showing all the Important Events** (Courtesy of RTD)

(a) Lateral Wave
(b) Diffraction of the Upper Defect Tip
(c) Diffraction of the Lower Defect Tip
(d) Reflection at the Back Wall
(e) Signal Caused by the Mode Converted Wave

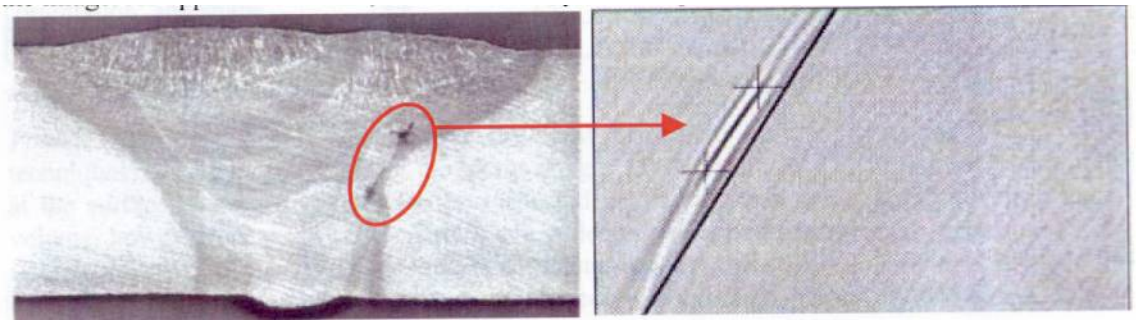

Figure 1.2-29. **Multi SAFT Image (Right) Showing the Result of the LOF Defect (Left)** (Courtesy of Maarten Lorenz – Shell Global Solutions International)

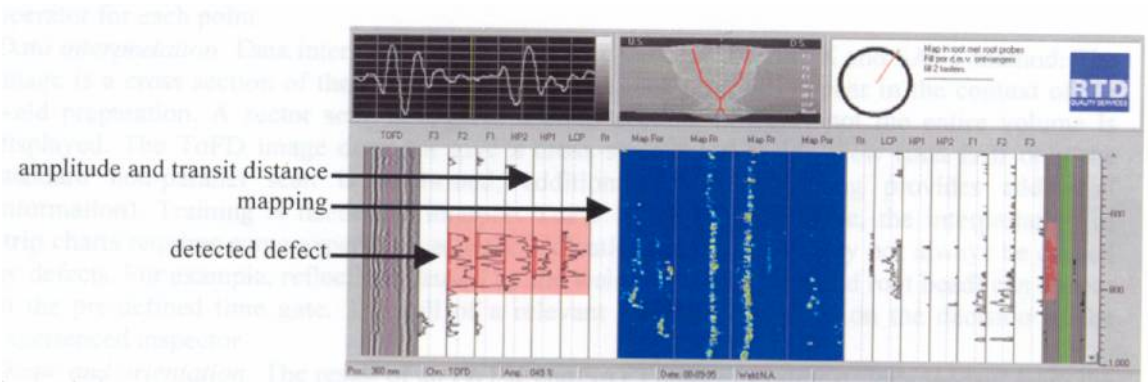

Figure 1.2-30. **Strip Chart Display** (Courtesy of RTD)

Results

A summary of the performance of different techniques is as shown in Table 1.2-7. Brief descriptions of the factors mentioned in the table are:

- **Volume Coverage:** A sector scan has least coverage as all the beams originate from only one point at the surface. TOFD covers larger area but has dead zones near the surface. The volume coverage of the IWEX method is complete, because effectively a focal spot is made for each point in the volume. SAFT offers complete coverage except when there are two defects blocking each other and thus making difficult for the ultrasound to reach. Strip charts cover the area around fusion line while the rest of volume is covered by use of map gates display.

- **Inspection Speed:** Due to the amount of data collected, IWEX and SAFT has lower inspection speed compared to TOFD, sector scans, and strip charts.

- **Processing Speed:** TOFD, sector scans, and strip charts do not require any processing as the data is directly displayed. IWEX and SAFT do require processing before the image is displayed. The speed of the processing speed depends on the amount of preparation and desired resolution.

- **Data Interpretation:** Data interpretation is very transparent in cases of IWEX and SAFT which gives the cross section of weld. TOFD provides a side view so position of defect is not known and also it requires skilled operator to interpret the data. Sector scan also provides a cross section but with limited coverage. Strip chart interpretation requires skilled interpreters and also not all indications on chart are always defect (for example, the geometry caused reflection).

- **Shape and Orientation:** The result of IWEX and SAFT is almost independent from shape and orientation of the indication. Information is gathered from all possible sides in this case. Orientation and shape plays important role in TOFD as two different orientations can provide same image. Strip charts and sector scans are strongly dependent on the orientation of defect.

- **Accuracy:** For all techniques that size the defects based on arrival times rather than amplitude is dependent on frequency bandwidth of the signal. This accuracy can be reached if all other parameters such as wedge angle, element spacing, and bandwidth are optimized and if parameters such as probe position, sound velocity, and wall thickness are accurate. A variation in parameters can cause variations in the arrival times and thus in the image. For IWEX and SAFT, the image will become blurry because the arrival times for compensation are out of focus. However, in terms of resolution, IWEX images can approach the physical limits better then other methods under practical conditions. Defect sizing for strip chart is partly based on amplitude by comparing the response from standard calibration reflector. No direct sizing relations can be used for data in map gates, because of the orientation of shape of porosity and slag inclusion which are usually different from the calibration reflector.

Table 1.2-7. Comparison of Different Imaging Techniques

	IWEX	TOFD	SAFT	Sector Scan	Strip Chart
Volume Coverage	++	+	++	-	+
Inspection Speed	+	++	-	+	++
Processing Speed	+	++	+	+	+
Data Interpretation	++	-	+	+	-
Orientation and Shape	++	+	+	-	-
Accuracy	+	+	+	+	+/-

Study 10 – Ultrasonic Inspection of Pipeline Split-Tees[1.2-31]

General

Pipeline repairs carried out on gas transport pipeline is performed in operational mode and thus demands high level of criticality during various stages like optimized welding procedures and consumables. It also makes it very important for ultrasonic testing to provide the right information about the weld quality, if the system used for testing is too sensitive in that case it would require for unnecessary repairs that are dangerous to be performed.

To improve the quality level of UT on split-tee fillet welds, a computer modeling study was initiated.[1.2-31] This study was split into two phases as mentioned below:

- Modeling performance of UT based on conventional probes as a function of geometry, defect type/size, and probe angle; this part of the study was then compared to practical experiments performed on the weld to validate the model.

- Using the model to optimize NDT parameters.

The reviewed content includes the results of Phase 1 only as Phase 2 study was not completed. The model used in the study is based on a finite difference scheme, this is an elastic model and takes into account all possible reflected and mode converted signals that can occur during travel of an ultrasonic wave front through solid material. Simulation parameters used for the study are as follows:

- Two typical geometries, within the boundaries of visually acceptance were selected (“ideal” and “irregular”).

- Two typical sleeve thicknesses were chosen (10 and 18 mm).

- UT probe parameters derived from standard angle transducers of 45, 60, and 70 degrees (4 MHz).

- LOF-type defects in the fusion line between repair sleeve and weld with varying heights as well as underbead defects at the toe of the weld and slag-shaped defects.

Figures 1.2-31 and 1.2-32 shows the parameters used for the study on a 10-mm sleeve and geometric parameters and defect types, respectively.

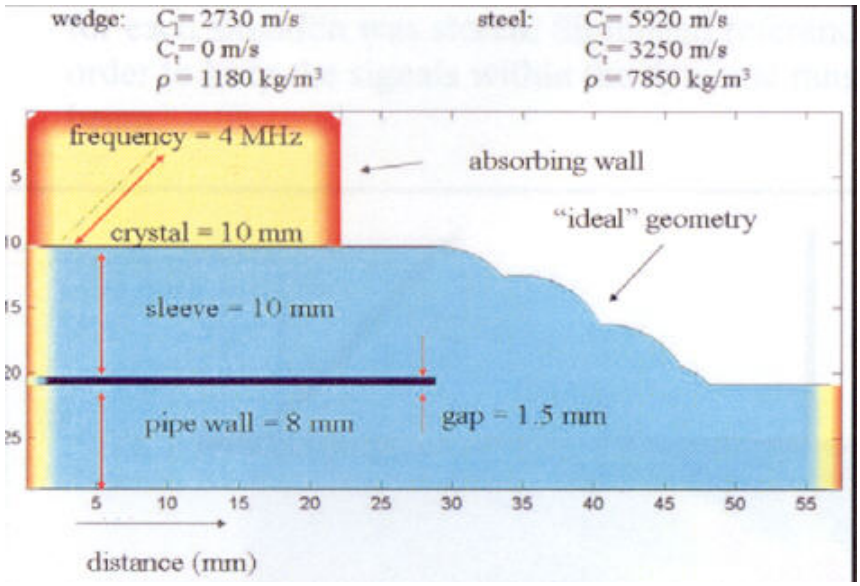

Figure 1.2-31. **Ultrasonic and Material Parameters** (Courtesy of RTD)

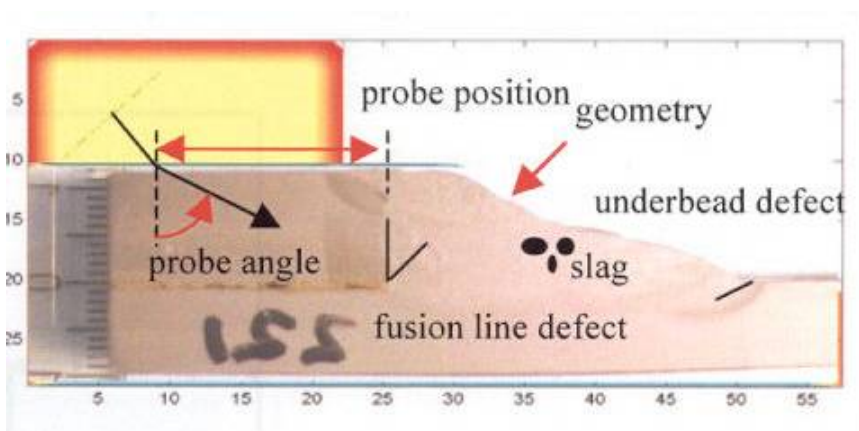

Figure 1.2-32. **Geometric Parameters and Defect Types** (Courtesy of RTD)

The inspection of four representative repair sleeve fillet welds with 10- and 18-mm sleeve thicknesses was carried out by five operators. The welds were then examined by radiographic testing.

Modeling Results

Indications of fusion defects at the vertical fusion line (between sleeve and weld) appear where no geometrical echoes are detected thus good detection of defects in this region. Figure 1.2-33 shows the wave front generated by the crystal is just about to hit the fusion defect. Part of the ultrasonic energy at this point has already been reflected back against the gap between sleeve and pipe wall. The blue color is compression waves while red is shear wave in figures.
Figure 1.2-34 the signal has just hit the crystal, reception has just taken place, and an A-scan has been detected with a good S/N ratio.

Figure 1.2-33. Wave Front is about to Hit Defect (Courtesy of RTD)

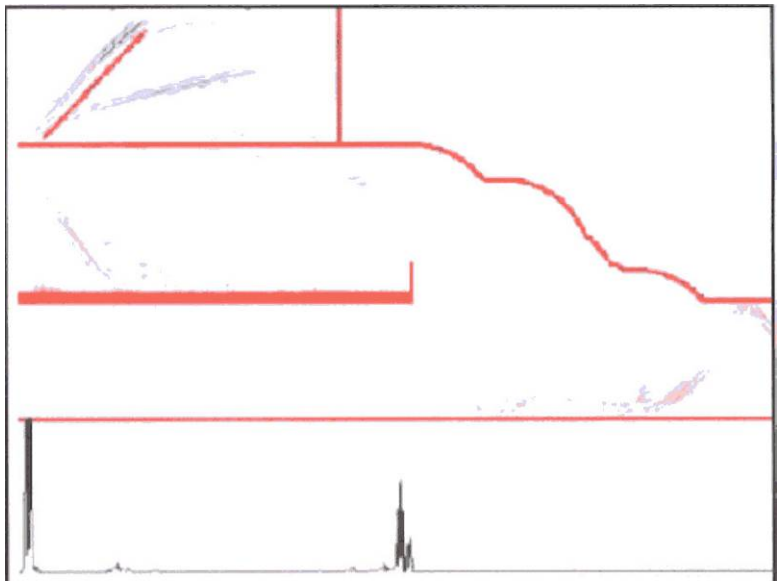

Figure1.2-34. Reflected Wave Front Just Hit Crystal (Courtesy of RTD)

On vertical fusion defects good relationship was between defect height and amplitude for defects up to approximately 4 mm. Above 4 mm the amplitude is saturated and on defects higher than 6 mm, even reduced. Due to this fact the defect size 8 mm and up gives amplitude that is comparable to 3 mm especially when 60- and 70-degree probes are used. Thus, discrimination between defects sizes becomes very difficult. This is shown in Figure 1.2-35, which is the result of a series of simulations whereby defect height was increased in 2-mm increments and the amplitude for each situation was stored.

Reflection against the gap between sleeve and pipe wall, and subsequently against the weld cap and back, generates a clear signal if no significant fusion defect is originating from the gap. As soon as defect height approaches 2 mm this geometric signal disappears. By the virtue of this benchmarking is possible for defect size.

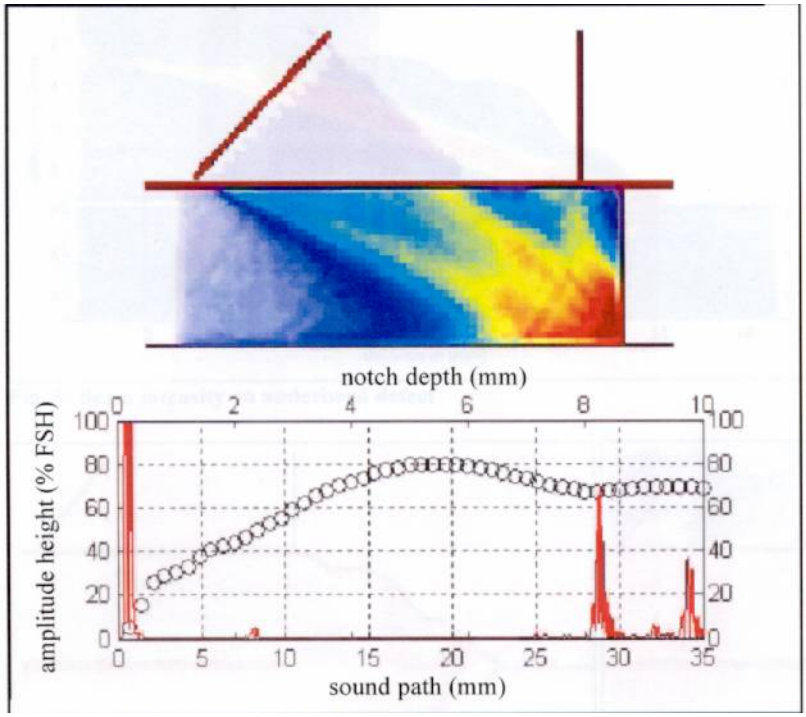

Figure 1.2-35. Amplitude as a Function of Defect Height – Fusion Defect, Corner Effect (Courtesy of RTD)

Figure 1.2-36 shows a simulation on an underbead crack at the weld's toe under a 45-degree angle, detected through the weld using a 70-degree probe placed on sleeve. Figure 1.2-37 shows the situation where the wave front has passed the crystal after reflection from defect and the A-scan shows (second echo, black) with amplitude that is approximately 6 dB lower than the reference echo (first echo, red). The reference echo in this case is established to 80% FSH using a 2-mm-high notch. Figure 1.2-38 shows the wave front before it hits the defect. This type of simulation showed that this is a good way to detect underbead cracks at the weld's toe, without significant influence of the (varying) weld geometry as long as it is within visual inspection acceptance limits. Sensitivity in this case has to be slightly higher than 80% FSH on a 2-mm notch.

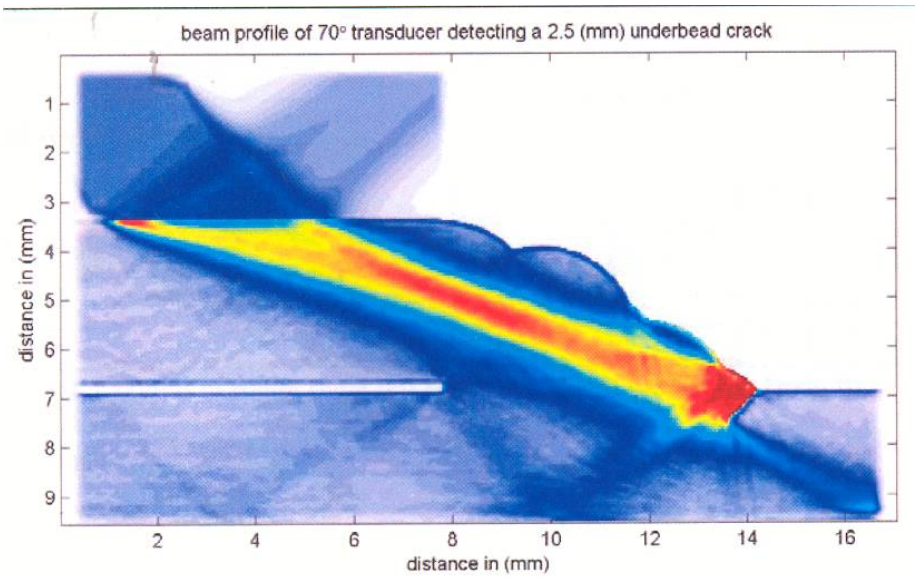

Figure 1.2-36. **Beam Intensity on Underbead Defect** (Courtesy of RTD)

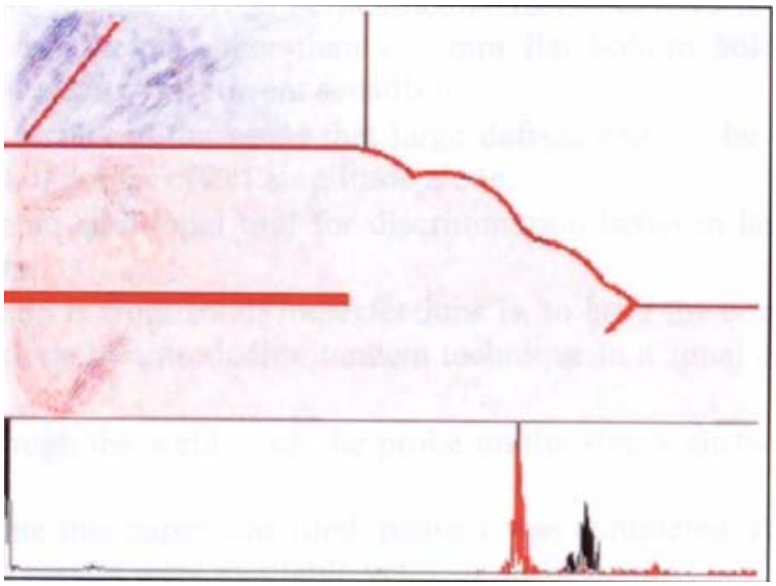

Figure 1.2-37. **Reflected Wave Front Just to Hit Crystal** (Courtesy of RTD)

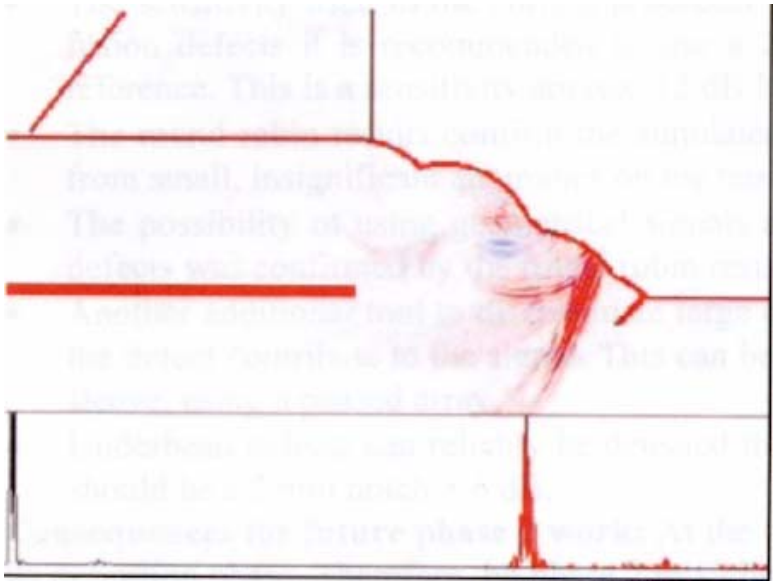

Figure 1.2-38. Wave Front just about to Hit Defect (Courtesy of RTD)

Test Results

Thin sleeves: Fusion defects with a 4-mm height and up were detected with POD of 92%. Length was on average overestimated by 23 mm, standard deviation of length inaccuracy was 19%.

Thick sleeves: Defects with 8-mm heights and up were detected with POD of 80% with considerable length overestimation.

UT picks up some non-relevant welding-related imperfections especially in the area of gap between sleeve and pipe and thus resulting in many unnecessary repairs.

Defect sizing was fairly accurate for defects with heights up to 4 mm within ±1.7 mm compared to the fabrication data of the intended defects. These results were in unison with the simulations. Figure 1.2-39 shows a typical example of the round-robin tests on one of the weld.

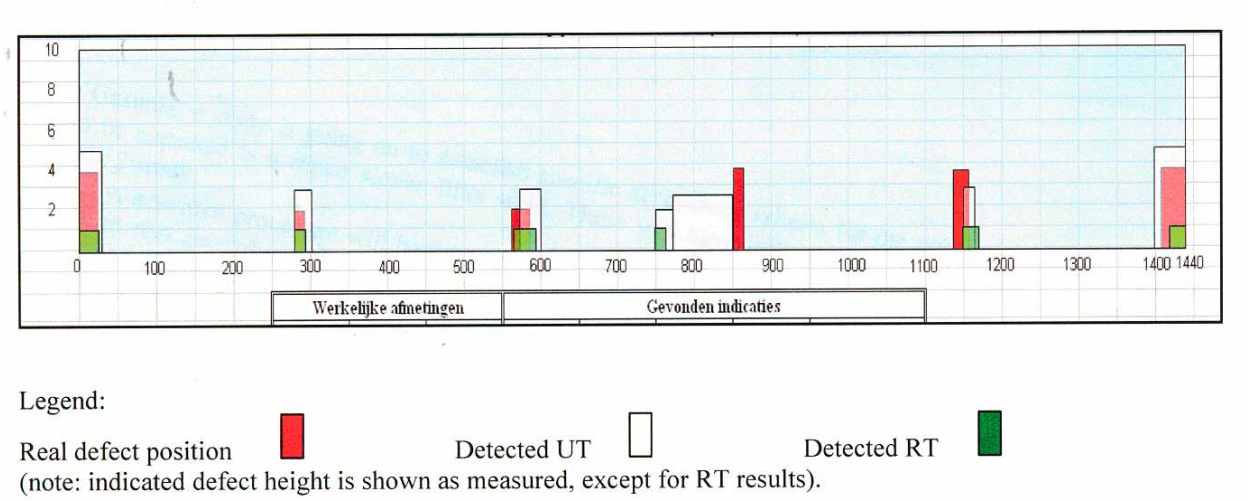

Figure 1.2-39. Example of Round-Robin Test Results on 10-mm-Thick Sleeve (Weld B) (Courtesy of RTD)

Conclusions

The sensitivity used in the current procedure for MUT on perpendicular fusion defects is too high. For fusion defects it is recommended to use a 2-mm notch rather than a 2-mm FBH in diagrams as a reference. This is a sensitivity approximately 12 dB lower than the current sensitivity.

The round-robin results confirm the simulated results cannot discriminate between the large and small defects, insignificant anomalies on the basis of corner effect amplitude.

The possibility of using geometrical signals as an additional tool for discrimination between large and small defects as confirmed from round-robin results.

Another additional tool to discriminate large defects from small imperfections is to have the complete area of the defect contribute to the signal. This can be done by using tandem techniques in a zonal concept on the sleeve, using a PA.

Underbead defects can reliably be detected through the weld, with the probe on the sleeve surface. Sensitivity should be a 2-mm notch + 6 dB.

Study 11 – Evaluation of TOFD for Search Scanning[1.2-32]

General

Recently, Mitsui Babcock performed a study to determine the extent to which defects can be missed when TOFD is used as a rapid NDT technique and as a stand-alone detection method in more realistic conditions.[1.2-32] Open and blind trials were carried on 20- to 60-mm-thick specimens with real and realistic flaws mainly fatigue cracks. The height of the flaws varied from 1.5 to 6 mm and the length from 5 to 150 mm. 58% of the flaws were in the root (mainly root cracks).

Test Results

Open trials demonstrated that certain types and locations of flaws are likely to be missed. Blind trials were performed by three companies in the facilities without knowing the objectives of the tests. A significant number of defects were missed or misinterpreted. A summary of the blind test results is shown in Table 1.2-8. The blind detection rates were from 26 to 42%. Detection rate was poor especially for root crack. None of the root cracks with reference height below 5 mm were detected. One of the four 5-mm height root cracks was not detected and from the three detected only one from the three teams interpreted the flaw as a root crack. The larger root crack with a 6-mm reference height was reported by only two teams and was dramatically undersized by both.

Table 1.2-8. TOFD Detection Blind Trial Results

Defect Type	Ref No.	Detected (0, 1, 2, or 3)	Defect Height (mm)			Defect Length (mm)		Obscuration[a]	Interpreted as
			Reference	Reported	Depth	Reference	Reported		
Root or inner surface cracks	1	3	5	3 4 5	17-20 15	30	400 150 32	M + P	Defect associate with root defect. Surface-breaking defect. Internal surface-breaking defect.
	3	3	5	3 6 6	17-20 14 14	30	400 27 30	M + P	Defect associate with root defect. Reflective signal. Internal surface-breaking defect.
	4	0	3.5	--	--	15	--	M + P	--
	9	0	5	--	--	30	--	M+ P	--
	12	2	6	4.5 4	30.5 31	30	35 42	NO	Indication. Internal surface-breaking defect.
	14	0	2	--	--	8 (28)	--	NO[b]	--
	16	2	5	3.5	36.5	15	20 11	NO	Disturbance at the back-wall. Internal surface-breaking defect.
Root defect	5	0	1.5	--	--	25	--	M	--
	7	0	2	--		15	--	M + P	--
	8	0	1.5	--		13	--	M + P	--
Mid-wall crack	19	2	6	3 3	13-16 15	50	45 14	P	Indication. Lack of side wall fusion.
Surface-breaking crack	2	0	3	--	--	15	--	M	--
	13	1	6	6.5	--	30	52	NO	External surface breaking.
Lack of side wall fusion	6	0	2.5	--	--	20	--	M	--
	10	1	2.5	4	--	10	15	P	LOF.
	11	2	2.5	-- --	23 30	5	6 20	P	Indication. Slag/porosity.
	17	3	5.5	 6.3 10	11-17 10.2-16.2 9	150	270 170 157	P + D	Lack of side wall fusion. Lack of side wall fusion. Lack of side wall fusion.
	18	0	5.5	--		50	--	D	--

Notes:
NO = No obscuration
P = Porosity
D = Other defect
M = Misalignment
(a) = Defects 12, 13, and 16 were offset from the weld centerline
(b) = The presence of backing plate may have been confusion

Conclusions

Even though TOFD is a good complimentary detection technique, there are conditions where it should not be used as a stand-alone NDE search method.

1.2.2.4 Pipeline Girth Weld and Repair AUT Inspection Methods – Summary

From the studies reported in the field of AUT it can be concluded that there are limitations and capabilities of each AUT system but there is also a lot of work carried out to overcome the limitations or to improve the capabilities of the AUT system.

Thus, it can be concluded that it is very important to understand the limitations and capabilities of the AUT system and select the right system required for the project. In addition, it is very important for AUT providers to work on overcoming the limitations and modify the system as and when required to meet the project criteria.

The above information proves that there has been a large effort put in by various parties to better understand the detection and sizing accuracy of AUT. The results have shown a variance in result from one study to another by some. The study performed suggested the need for a Global AUT qualification where all the systems are qualified to the same rules and the results laid out are officially accepted by right from the oil companies to the AUT contractors. This effort can also further lead into standardization of guidelines that can be used for system qualification and also lead to change in Codes requirement.

1.2.2.5 References

1.2-1. Lozev, M., “Validation of Current Approaches for Girth Weld Defect Sizing Accuracy by Pulse-Echo, Time-of-Flight Diffraction, and Phased Array Mechanized Ultrasonic Testing Methods”, Final report, PRCI Contract No. GRI-8369 and EWI Contract No. 45800-IRD (July 2002).

1.2-2. Spencer, R., "Ultrasonic Detection Limits for Cracks in Carbon and Stainless Steel Welds - A Literature Review", EWI Project No.43312 CAP, PV PVRC Project No. 99-NDE-01 (September 2000).

1.2-3. Doctor, S. R., Selby, G. P., Heasler, P. G., and Becker, F. L., “Effectiveness and Reliability of Inservice Inspection, a Round Robin Test”, *Proceedings of the Fifth International Conference on Nondestructive Evaluation in the Nuclear Industry* (May 1982).

1.2-4. Bowker, K. J., Chapman, R. K., and Wrigley, J. M., “Some Principles for the Design of High Performance Automated Defect Detection Systems”, Nondestructive Testing in the Fitness-for-Purpose Assessment of Welded Structures, International Conference (November 1984).

1.2-5. Silk, M. G., Stoneham, A. M. and Temple, J.A.G., “The Reliability of Nondestructive Inspection”, Adam Higer, Bristol (1987).

1.2-6. Taylor, T. T., Spanner, J. C., Sr., Heasler, P. G., Doctor, S. R., and Deffenbaugh, J. D., “An Evaluation of Human Reliability in Ultrasonic In-Service Inspection for Intergranular Stress-Corrosion Cracks through Round-Robin Testing”, *Materials Evaluation*, Vol. 47 (March 1989).

1.2-7. Cerri, M. and Cusolito, R., “Experiences in Capability Assessment of Manual Ultrasonic Examination Techniques for Planar Flaw Detection and Sizing in Austenitic Stainless Steel Joints”, NDT International (August 1989).

1.2-8. Nishino, S., Hida, Y., Yamamoto, M., Ando, T., Shirai, T., Enami, K., and Fukui, S., “Ultrasonic Testing of Austenitic Stainless Steel Welds”, *The Fourth International Symposium of the Japan Welding Society* (November 1982).

1.2-9. PISC II (Program for the Inspection of Steel Components) Report (September 1986).

1.2-10. Shackleton, D. N., Pattison, J.E.K., and Skirving, N., “Performance of Ultrasonic Inspection in Thick Walled Pressure Vessel Fabrication”, Nondestructive Testing in the Fitness-for-Purpose Assessment of Welded Structures, International Conference (November 1984).

1.2-11. Shannon, R.W.E, Jackson, L., and Morgan, L. L., “The British Gas Approach to Pipeline Monitoring”, Nondestructive Testing in the Fitness-for-Purpose Assessment of Welded Structures, International Conference (November 1984).

1.2-12. Raj, B. and Subramanian, C.V., “Research and Development Activities in Quality Assurance of Welded Components at Indira Gandhi Centre for Atomic Research”, *Indian Welding Journal* (October 1990).

1.2-13. Charlesworth, J. P. and Hawker, B. M., “Inspection of the Near-Surface Defect Plate (DDT3) by the Ultrasonic Time-of-Flight Technique”, *British Journal of Nondestructive Testing* (February 1984).

1.2-14. Stringfellow, M. W. and Perring, J. K., “Detection and Sizing of Inner Radius Defects in DDT Plate 4 (Simulated PWR Nozzle) by the Ultrasonic Time-of-Flight Diffraction Technique”.

1.2-15. Trimborn, N., “The Time-of-Flight Technique”, *NDTnet* (September 1997).

1.2-16. Lemaitre, P., Koble, T. D., and Doctor, S. R., “Main Results of the PISC III Capability Studies on Wrought-to-Cast Austenitic Steel Welds”, ASME (1995).

1.2-17. Davis, J. M., Advanced Ultrasonic Flaw Sizing Handbook, 1998 Edition.

1.2-18. Hands, G., “Automated NDT Advantages and Disadvantages”, *NDTnet* (March 1996).

1.2-19. Forli, O., “Qualification of AUT for Offshore Pipelaying and the Role of NDE Reliability”, 3rd European-American Workshop on Reliability of NDE and Demining, Berlin (September 2002).

1.2-20. Spencer, R., "Evaluation of Ultrasonic Sizing Methodologies and their Applicability to Cracking", EWI Project No. 426471RP (June 30, 2000).

1.2-21. Moles, M., "Defect Sizing in Pipeline Welds - What can we Really Achieve?”, *Proceedings of ASME PVP Conference*, San Diego, California (July 2004).

1.2-22. Heasler, P. G., and Doctor, S. R., ”Piping Inspection Round Robin”, NUREG/CR-5068, PNNL-10475 (1976).

1.2-23. Denys, R., Lefevre, T., de Jaeger, C., and Claessens, S., ”Study on Weld Defect Acceptance Criteria”, Final Report for Group of Sponsors, Laboratorium Soete, Gent, Belguim (2000).

1.2-24. Morgan, L., "The Performance of Automated Ultrasonic Testing (AUT) of Mechanised Pipeline Girth Welds", *NDT.net*, Vol. 8, No. 3 (March 2003).

1.2-25. Morgan, L. P., Nolan, P., Kirkham, A., and Wilkinson, P., ”The Use of Automated Ultrasonic Testing (AUT) in Pipeline Testing”, *Insight*, Vol. 11 (2003).

1.2-26. Kopp, F., Perkins, G., Stevens, D., and Prentice, G., "High-Resolution Sizing Capabilities Required for Automated Ultrasonic Inspection of Offshore Pipeline and Catenary Riser Welds", *Pipes and Pipelines International*, Vol. 46, No. 3 (May-June 2001).

1.2-27. Cataldo, R. and Legori, R., ”Advanced Ultrasonic Techniques in Pipelines Girth Welds Examinations”, *ASME PVP*, Vol. 456, p. 49.

1.2-28. Ginzel, E, van Dijk, H., and Hoff, M., "TOFD Enhancement to Pipeline Girth Weld Inspection", *NDT.net*, Vol. 3, No. 4 (April 1998).

1.2-29. Moles, M. and Zhang, J., "Wall Thickness Compensation for Seamless Pipe Inspection Using Phased Arrays”, Final Report, Gas Research Institute, GTI-8766 (March 2005).

1.2-30. Pörtzgen, N., Dijkstra, F.H.D., Gisolf, A., and Blacquière, G., "Advances in Imaging of NDT Results", *16th WCNDT 2004-World Conference on NDT*, Montreal, Canada (August 30-September 3, 2004).

1.2-31. Dijkstra, F. H., Pörtzgen, N., and van Merriënboer, H.A.M., "Ultrasonic Inspection of Pipeline Split-Tees", *16th WCNDT 2004-World Conference on NDT*, Montreal, Canada (August 30-September 3, 2004).

1.2-31. Farley, J. M., Goujon, N. S., and Sheperd, B.W.O., ”Critical Evaluation of TOFD for Search Scanning”, *16th WCNDT 2004-World Conference on NDT*, Montreal, Canada (August 30-September 3, 2004).